

Modelling and Control of Wind Turbines, Solar Photovoltaic and Electric Vehicles in Residential Grids

by

Brindusa Bogdan Mihai

Aalborg University

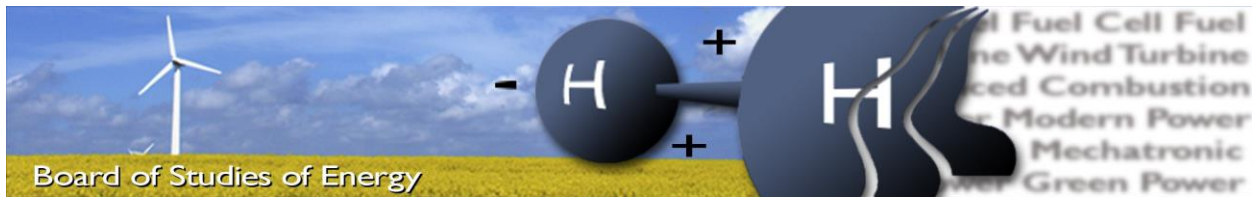
Department of Energy Technology

Group: EPSH3-934

Date: 5th of January 2018



AALBORG UNIVERSITY
DENMARK



Title: [Modelling and Control of Wind Turbines, Solar Photovoltaic and Electric Vehicles in Residential Grids]
Semester: [4]
Semester theme: [Master's Thesis]
Project period: [2nd of February – 5th of January]
ECTS: [50]
Supervisors: [Weihao Hu, Chi Su]
Project group: [EPSH4-934]

Bogdan Mihai Brindusa

SYNOPSIS:

The predictions regarding the energy trends are showing that by 2050 Denmark should be fossil-fuel independent. Renewable generation being hardly predictable, the need of storing the energy in periods of extra generation, occurs. The main aim of this master thesis is to determine the maximum renewable generation that can be integrated in the system, using Heat Pumps and Electric Vehicles, as variable loads. Firstly, the validation of the IEEE 13 bus network is achieved, in order to have a suitable benchmark for the upcoming studies. Secondly, the maximum renewable generation is found by gradually increasing the integration level, for both January and July until one of the critical limits is reached. Furthermore, active and reactive power control methods are used to increase even further, the maximum renewable generation. Finally, a techno-economical study regarding the charging methods of the Electric Vehicles is studied, determining the profit the EV owners could benefit.

Pages, total: [91]
Appendix: [1]
Supplements: [-]

By accepting the request from the fellow student who uploads the study group's project report in Digital Exam System, you confirm that all group members have participated in the project work, and thereby all members are collectively liable for the contents of the report. Furthermore, all group members confirm that the report does not include plagiarism.

List of abbreviations

EVs	Electric vehicles
V2G	Vehicle-to-grid
G2V	Grid-to-vehicle
HP	Heat pump
DSO	Distribution System Operator
TSO	Transmission System Operator
PVs	Photovoltaic panels
LV	Low voltage
MV	Medium voltage
DPL	Digital programming language
WT	Wind turbine
HV	High Voltage

Contents

List of abbreviations	3
List of Figures	7
Summary	9
1 Introduction.....	10
1.1 Background and motivation	10
1.1.1 Wind Power	11
1.1.2 Solar Power.....	12
1.1.3 Electric Vehicles	14
1.1.4 Heat Pumps	17
1.2 Danish Electricity Sector.....	18
1.3 Danish Smart Grid.....	19
1.4 Electricity market in Denmark	21
1.4.2 Regulating power market.....	21
1.4.3 Balancing Power	22
1.4.4 Elspot – Nord Pool Spot’s Day-ahead Auction Market.....	22
1.5 Project Objectives	23
1.6 Methodology	24
1.7 Limitations	25
1.8 Outline of the thesis.....	25
2 Description and validation of the system.....	27
2.1 Power Flow Analysis	27
2.1.1 Voltage Controlled Bus.....	28
2.1.2 PQ Bus (Load Bus).....	29
2.1.3 Slack Bus	29
2.1.4 The Bus Admittance Matrix.....	29
2.2 IEEE 13 bus distribution system validation	33
2.3 Summary	36
3 Modelling of the generation and consumption profiles	38
Summary.....	40
3.1 Wind Turbines Power Simulation.....	42
3.2 Photovoltaic Panels Power Simulation	43

3.2.1	Total tilted irradiance calculation	44
3.2.2	PV cell temperature calculation	46
3.3	Heat Pump Power Demand	47
3.4	Electric Vehicle Integration	49
3.4.1	Number of EVs	49
3.4.2	Driving Distance	50
3.4.3	Charging power levels	50
3.4.4	Charging Profiles	51
3.4.5	Consumption needed for EVs	51
3.5	Summary	52
4	Maximum Allowable Renewable Integration with and without Heat Pump Integration	53
4.1	Household consumption.....	54
4.2	Maximum Renewable Integration.....	55
4.2.1	January Case	55
4.2.2	July Case	60
4.3	Integration of Heat Pumps in the system	64
4.4	Summary	66
5	Control Methods to Increase Maximum Allowable Renewable Integration	68
5.1	Active Power Control.....	68
5.2	Reactive Power Control	73
5.3	Summary	76
6	Technical-Economic Analysis	78
6.1	January Case.....	78
6.1.1	Dumb Charging.....	78
6.1.2	Smart Charging	81
6.2	July Case	84
6.3	Economic Analysis.....	86
6.3.1	January Case	86
6.3.2	July Case	87
6.4	Summary	87
7	Conclusion	89

8	Future Work	91
	Bibliography	92
	Appendix 1	94

List of Figures

Figure 1-1 Installed RE Capacity in Europe [MW] 2000-20016 [3]	11
Figure 1-2 Installed Wind Capacity in Denmark [3]	11
Figure 1-3 Wind Turbines by Capacity in Denmark [4].....	12
Figure 1-4 Installed Capacity of Photovoltaic Panels in Denmark [3]	13
Figure 1-5 Number of PVs in Denmark [4]	13
Figure 1-6 Comparison of the costs of ownership of EVs compared to Petrol and Diesel Vehicles [10].....	16
Figure 1-7 Expected Future EV share [8]	16
Figure 1-8 Heat Pump Cycle [14].....	17
Figure 1-9 Challenged in Distribution Grids [7].....	18
Figure 1-10 Illustration of the Elements of a Danish Smart Grid [20]	20
Figure 1-11 The commercial players and the electricity exchange [21].....	21
Figure 1-12 Price setting in the regulating power market [21]	22
Figure 1-13 Supply Demand per one day [21].....	22
Figure 2-1 Load Flow Parameters.....	27
Figure 2-2 Transmission Line Model	28
Figure 2-3 PV Bus	28
Figure 2-4 Load Bus Model.....	29
Figure 2-5 Simple 4 Bus Network	30
Figure 2-6 Simple 4 Bus Network with variables [19]	30
Figure 2-7 Bus Admittance Diagram.....	31
Figure 2-8 IEEE 13 Bus Test Network [25]	33
Figure 2-9 DigSilent PowerFactory 13 Bus Network.....	34
Figure 3-1 Wind power generation and household electricity consumption for January and July41	
Figure 3-2 Wind Speed vs Power Curve for Osiris 10 turbine	42
Figure 3-3 Wind Speed and Wind Power Generation for 1 day in January/July.....	43
Figure 3-4 PV Power Generation July and January	47
Figure 3-5 The Lift [59].....	48
Figure 3-6 COP vs Lift [30].....	48
Figure 3-7 Thermal Energy vs Electrical Energy	49
Figure 3-8 Average daily driving distance in DK [32]	50
Figure 4-1 The Critical Components of the system	53
Figure 4-2 Household Electricity Consumption January/July 2013	55

Figure 4-3 Max Renewable Cases 1-4 January.....	57
Figure 4-4 Node 675 Voltage Levels January	58
Figure 4-5 Transformer Loading January	58
Figure 4-6 Line Loading January Case	59
Figure 4-7 Max Renewable Generation (WT+PV) January	60
Figure 4-8 Maximum Renewable integration July	61
Figure 4-9 Transformer Loading in July.....	62
Figure 4-10 Node 675 Voltage in July.....	63
Figure 4-11 Lines Loading July	64
Figure 4-12 Renewable Maximum Generation July.....	64
Figure 4-13 New Maximum Renewable Generation January.....	65
Figure 4-14 Old vs New Generation January	66
Figure 5-1 Active Power Control Flowchart	69
Figure 5-2 Max WT January.....	70
Figure 5-3 Voltage, Transformer and Line profiles for 850 WTs (January)	71
Figure 5-4 Max WT July (600 WTs)	72
Figure 5-5 Voltage, Transformer and Main Line profiles for 600 WTs (July).....	73
Figure 5-6 Reactive Power Control profiles (January).....	75
Figure 5-7 Reactive Power Control (July)	76
Figure 6-1 Simulation Method of EV Charging	79
Figure 6-2 Dumb Charging January	81
Figure 6-3 Loading difference between the Main and Second Transformer	82
Figure 6-4 Smart Charging Profiles	84
Figure 6-5 Dumb charging profiles- July.....	86

Summary

Renewable Generation such as Wind Power Generation as well as Solar Power Generation, is on a continual rise. Relying this much on renewable integration, may stress the system, and also generate unbalances in the system. Methods to store the extra energy when the production is bigger than consumption (especially in the night). Loads such as Electric Vehicles and Heat Pumps.

In this master thesis, the renewable integration is modelled and raised to the maximum capability that the system can support, regarding its limits. The system is modelled and validated on the IEEE 13 Bus Network. Furthermore, Heat pumps are integrated as well into the system, in order to increase the consumption, during the off-peak household consumption hours. After the integration of heat pumps, the number of wind turbines possible to operate in the system, increases by 10 times.

Control Methods are further analyzed, to increase even more the renewable generation that can be integrated into the system. Active Power Control consists of lowering the power production in the periods where the system limits may be violated.

Another type of control, analyzed in this project, is the reactive power control, based on generating or consuming reactive power in order to keep the system in its established limits. By doing this method, the maximum number of Wind Turbines and PV panels are found.

Finally, different charging strategies are studied, in order to find the highest profit for the EV owners, while keeping the system under the limits.

1 Introduction

A study made by the Global Sustainability Institute shows that a significant number of countries face severe shortage of fossil fuels [1]

Denmark is one of the countries which promotes renewable energies. The main goal regarding this aspect is to become fossil fuel independent by 2050. Denmark is currently producing approximately 25% of its energy from wind and is aiming for a 50% wind share of energy production by 2025 [2]. Solar energy is also coming to a rise in the last years, with many residential consumers installing them in their houses.

On the other hand, due to the high wind and solar penetration, EVs and Heat pumps can be used to lower the excess power in the high peak periods. Electric Vehicles not only that are fossil fuel free, but they also can use their battery and can act when connected to the network as a controllable load and also as an energy storage device (Vehicle-to-grid V2G or Grid-to-Vehicle G2V).

Heat pumps are as well fossil fuel independent which makes this combination (HP-EVs) to be taken into consideration in order to achieve faster the goal of being fossil fuel independent. As well as the EVs, heat pumps can store electric energy as heat from the excess energy generated by the wind turbines and photovoltaic panels.

1.1 Background and motivation

Renewable energy interest increased tremendously compared to the previous years in Europe. According to IRENA (International Renewable Energy Agency), the installation capacity on renewable energy in Europe in the last years increased significantly, reaching more than double capacity in 2016, 486 MWe, compared to year 2000 where there were installed only 186 MWe. This rapid increase can be seen in Figure 1-1.

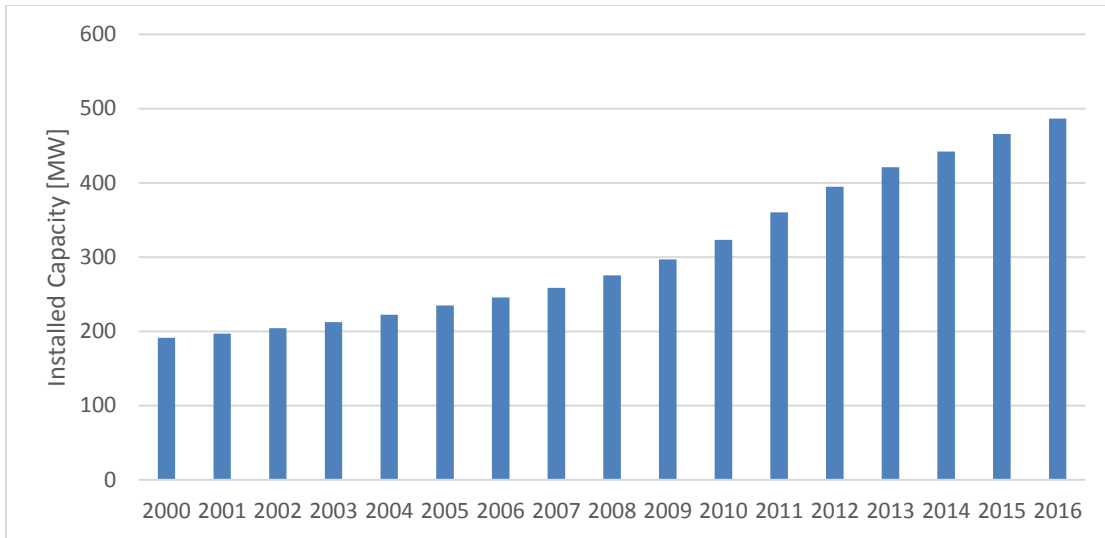


Figure 1-1 Installed RE Capacity in Europe [MW] 2000-2016 [3]

1.1.1 Wind Power

Regarding Denmark, it is well known that it has been a leader in wind power production, reaching 42.1% of the total power produced in 2015 just from wind. In 2012, the Danish government developed a plan to increase the share of electricity from wind to 50 % in 2020, and to 84% in 2035 [2]. The on-shore and off-shore wind power production can be seen in Figure 1-2.

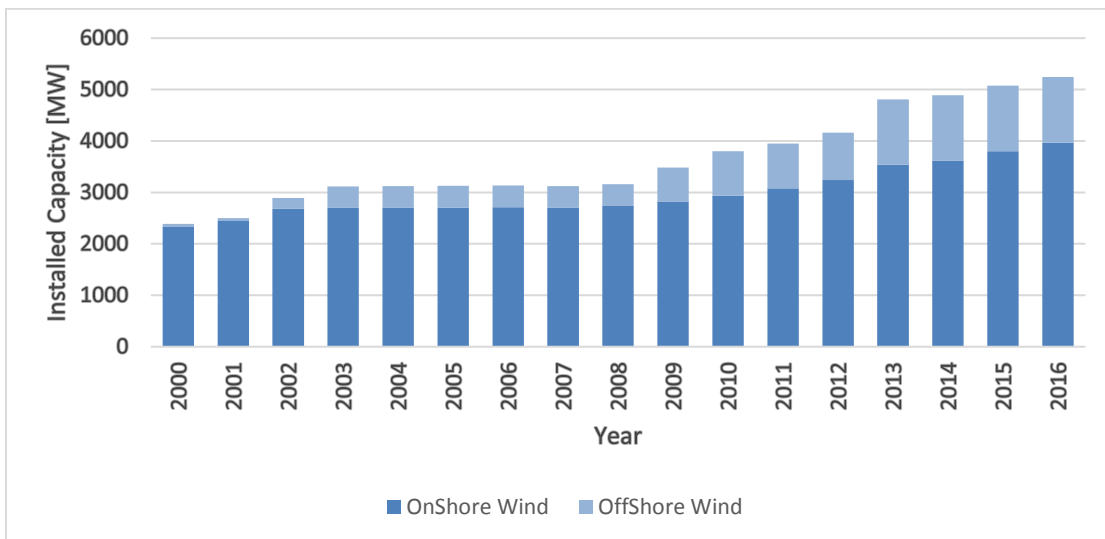


Figure 1-2 Installed Wind Capacity in Denmark [3]

As it can be seen in Figure 1-2 the annual wind power installation is on a continuous rise, having 5024 MW installed in 2016 compared to 2339 MW installed in 2000.

In order to promote even more installation of wind turbines, the Transmission System Operator (TSO), Energinet.dk offers to pay the consumers who install wind turbines for 12 years. For wind turbines smaller than 10 kW the revenue will be of 212 øre/kWh and for wind turbines with a capacity between 10-25 kW it will be of 132 øre/kWh. [4]

Figure 1-3 illustrates the number of currently operating wind turbines in Denmark in 2016 of various powers.

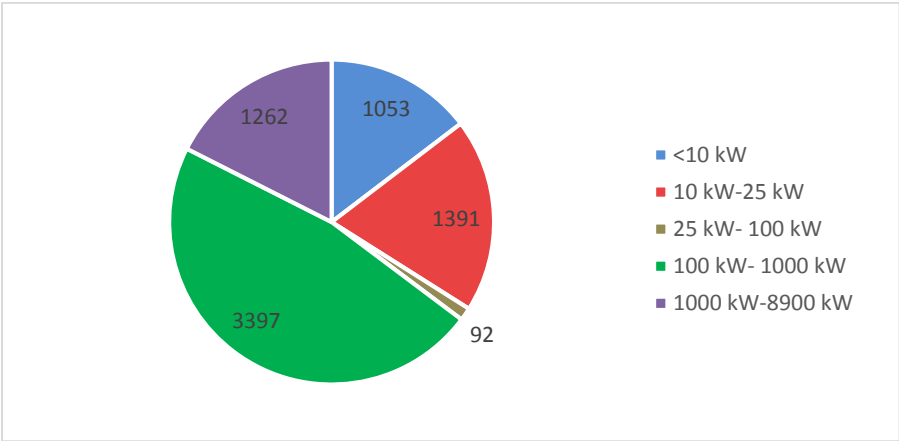


Figure 1-3 Wind Turbines by Capacity in Denmark [4]

For wind turbines, subsidies constituting 4.5 billion DKK have been paid in 2015 [5]

1.1.2 Solar Power

Another resource which progressed significantly by means of installed capacity in Denmark is solar power.

It can be seen in Figure 1-4, the solar power increased exponentially from almost none in the period of 2000-2011 to 790 MW in year 2016.

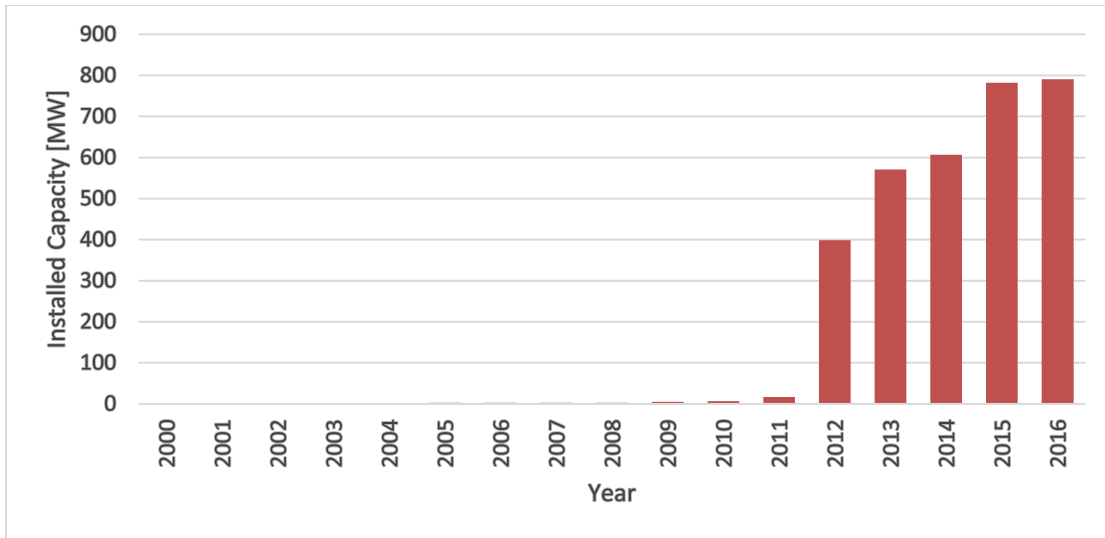


Figure 1-4 Installed Capacity of Photovoltaic Panels in Denmark [3]

According to Energinet.dk, the installed capacity of PVs should reach to 2 115 MW in 2025, three times larger than the current state, and it is estimated that they will produce 1.950 GWh, which is equivalent to 5% of the total electricity consumption, making it a resource which should be analyzed thoroughly. By 2013, the government implemented a new regulation in which it encourages the installation of PV for net-metering scheme with 60 øre/kWh for first 10 years and to 40 øre/kWh for the following 10 years.

In Figure 1-5 it is presented the number of currently working PV's in Denmark under various powers, with the small panels (under 6kW) being the majority.

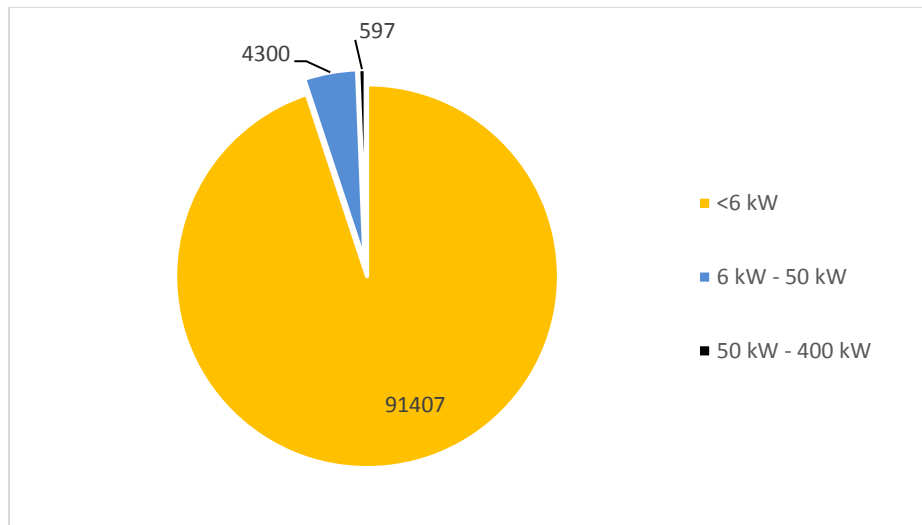


Figure 1-5 Number of PVs in Denmark [4]

For solar cells, subsidies constituting 74 million DKK have been paid in 2015 [5]

As it has been seen previously, wind and solar power are quite expanding at a rapid rate. Having also the financial support from TSO for the consumers will lead to a change in system, from a more centralized generation power plants, which are usually based on fossil fuels, to a more distributed generation power plants based on renewable energy [6].

In this Project, January and July were taken as the months where the studies are done. These months are representative for the higher consumption in January (Winter case) due to the heating and lightening, and also high wind speeds. Where, compared to July where there are the periods of the lowest consumption in the year, together with lower wind speeds, but much more solar power.

1.1.3 Electric Vehicles

Electric vehicles are based on getting the power from an electric motor instead of a gasoline engine. These Electric Vehicles can range from electric trains, boats, to electric cars.

By the year of 1830, the first electric vehicles were starting to be used for transportation. They were considerably different from the electric vehicles known today, mainly because they didn't use rechargeable batteries. The first electric vehicles with proper rechargeable batteries, started to be produced by 1859 [7]. Around 1900, electric vehicles became widely known and used around the world [8]. However, due to the discoveries made in the oil field, which also took place at around the same time, making the oil extremely cheap and accessible everywhere, made the industry to change its attention to gasoline engines [20]. At the end of the 20th century the electric vehicles regained their popularity due to the fossil fuel shortages, gas emissions and also transportation regulations.

Compared to the conventional vehicles, EVs have the following advantages [8]

- **Energy Efficiency:** The conversion of electrical energy from the grid to the wheels is around 59%-62%, compared to gasoline powered vehicles which can convert up to a maximum of 17-21% of the energy which is stored in gasoline to the wheels.
- **Performance:** Electric Motors provide a smooth and quiet operation, with greater acceleration and also, they require less maintenance compared with the conventional combustion engines.
- **Environmental Factors:** Even though conventional gasoline engines have reduced their emissions in the last years, they are still one important factor in the high percentage of Greenhouse Gas Emissions generated around the world. On the other hand, EVs have zero pollutant emissions.

- Encouragement Governmental Plans: In order to motivate the public into purchasing an electric vehicle, and not a conventional one, Governments throughout the world are supporting economically the people which are buying EVs by lowering the taxes for them, even by 50%. For example, in Copenhagen, electric cars have free parking places. [9]
- Solving high wind and solar power penetration: In the periods when there is excess power from renewable sources, Electric Vehicles can be recharged in order to use the power efficiently. Furthermore, there can be made an optimization plan with the DSO (Distribution System Operator) to recharge when it is more suitable economically as well as safe for the grid.

Even though EVs are rising in popularity at an extreme rate, there are still quite challenges when buying an EV [10]:

- Driving Range: The range of a normal EV is 100-200 km. Although there are some models which can reach 300-400 km with a fully charged battery.
- Battery Cost: Depending on the size of the battery, the price is quite high, and throughout the life of the car, the battery may have to be replaced a couple of times.
- Recharging Times: A full recharge of the battery can take up to 4-8 hours, depending of the size of the battery.
- Noise Awareness: Although the quiet sound produced by EVs is a plus, regarding the safety issues it may be a disadvantage.

In Europe, the fuel prices in the last years, have been significantly higher than in North America. As it can also be seen in Figure 1-6, the costs of owning an EV is lower than owning a conventional vehicle.

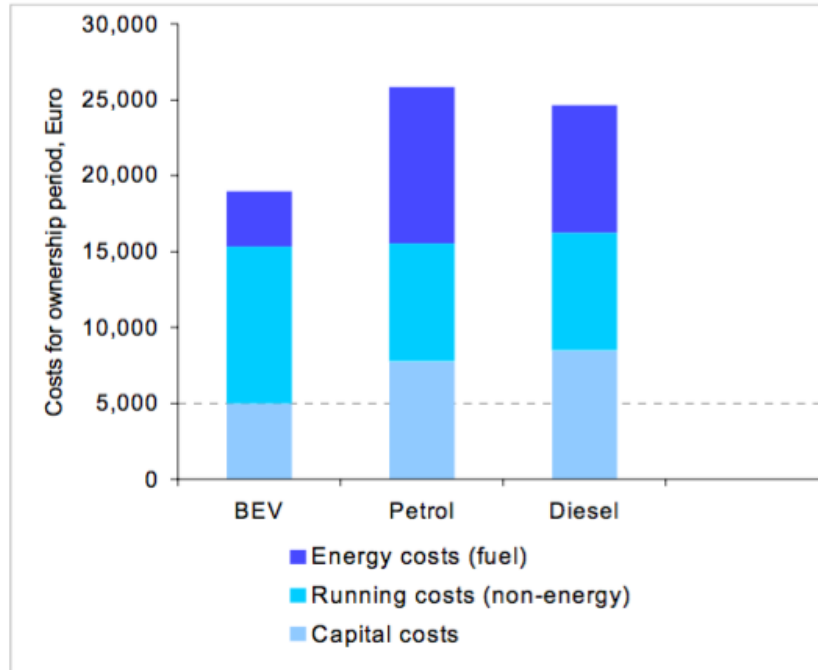


Figure 1-6 Comparison of the costs of ownership of EVs compared to Petrol and Diesel Vehicles [10]

With the upcoming popularity of EVs and also because of the national energy policies and charging infrastructure, the EVs are expected to grow from around 37 000 EVs in 2012 to an astonishing 669 000 electric vehicles in 2020 according to [11]

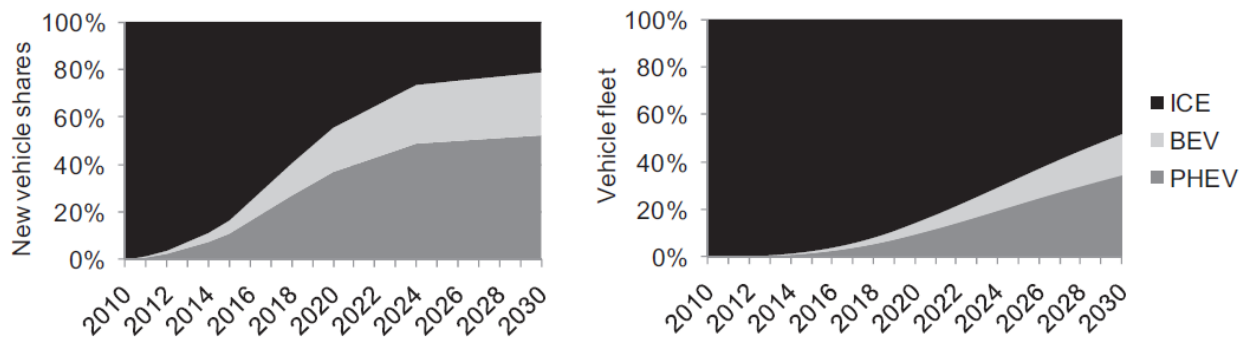


Figure 1-7 Expected Future EV share [8]

As shown in Figure 1-7, the EVs will massively increase in the new vehicle market shares, reaching around 80% of the new vehicles by 2030. This prediction may materialize, according to [12] which shows companies like Volvo who will stop designing conventional vehicles by 2019. Furthermore, Mercedes announced that from 2022 it will produce only electric and hybrid vehicles. Another reason to understand that this trend will arise at an exponential rate is that in

2016 Germany's Bundesrat, which is the federal council, passed a resolution forbidding conventional vehicles by 2030 [13]

Currently, 20% of the total cars are electric vehicles, according to Figure 1-7. This assumption will be further utilized in the project.

1.1.4 Heat Pumps

Another type of load to be used in a smart grid, solving the problem of high wind and solar penetration is heat pump. In 2010, the Danish Energy Association announced that 300 000 heat pumps will be installed in Denmark by 2025. In Figure 1-8 the cycle of an air-air heat pump is presented.

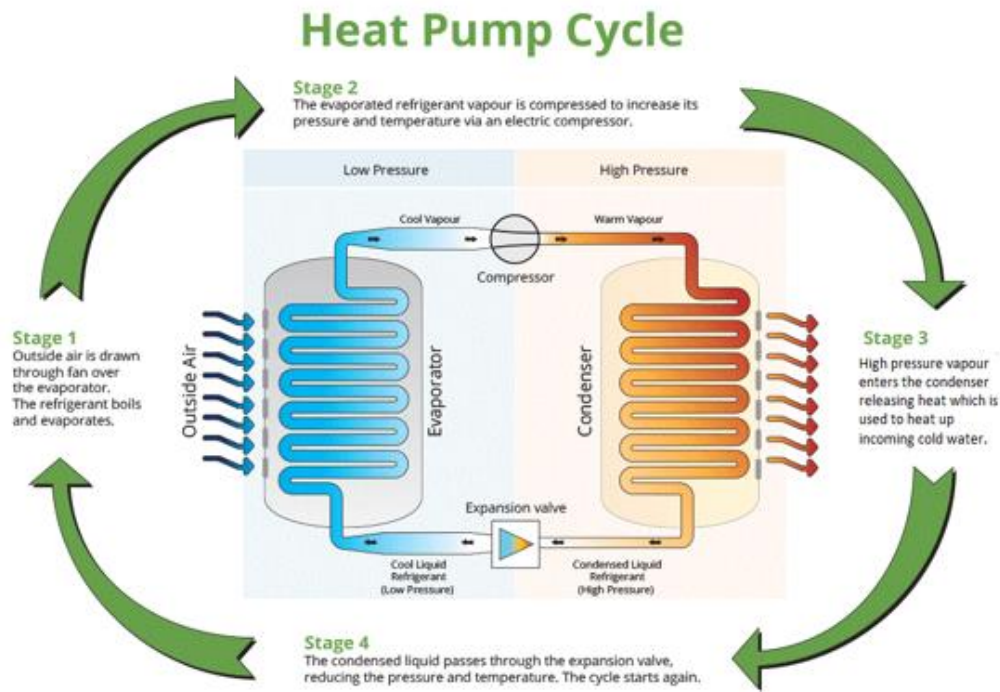


Figure 1-8 Heat Pump Cycle [14]

Because of their flexibility potential and their capability to balance the high wind penetration, an increasing number of research on heat pumps shows the rising interest for this technology in Denmark [14]. [15]The principle on which a heat pump works is based on the fact that the electricity needed to provide a certain amount of thermal energy is always lower than the thermal energy provided, which makes them viable for implementing in homes.

The most common type of heat pump is the air-source heat pump, which transfers heat between to the house and the outside air. Today's heat pump can reduce the electricity use for heating by

approximately 50% compared to the conventional electric resistance heating [30]. For example, [16] found that if a conventional heater (electrical resistance) is replaced with an air-source heat pump, the annual savings are around 3000 kWh (6360 DKK). The same heat pump was compared with an oil system and the savings resulted as 6200 kWh and (13144 DKK). Also predicts that by 2030 there will be a 40% market penetration for air-air heat pumps. [16]

1.2 Danish Electricity Sector

More than 10 years ago, wind power plants could be disconnected from the grid during disturbances [7]. However, nowadays it is not possible to do so anymore. Due to the highly integration of wind power in the power system, new challenges emerge for the system.

In Figure 1-9 it is presented how the generation and consumption affect the voltage in terms of distance.

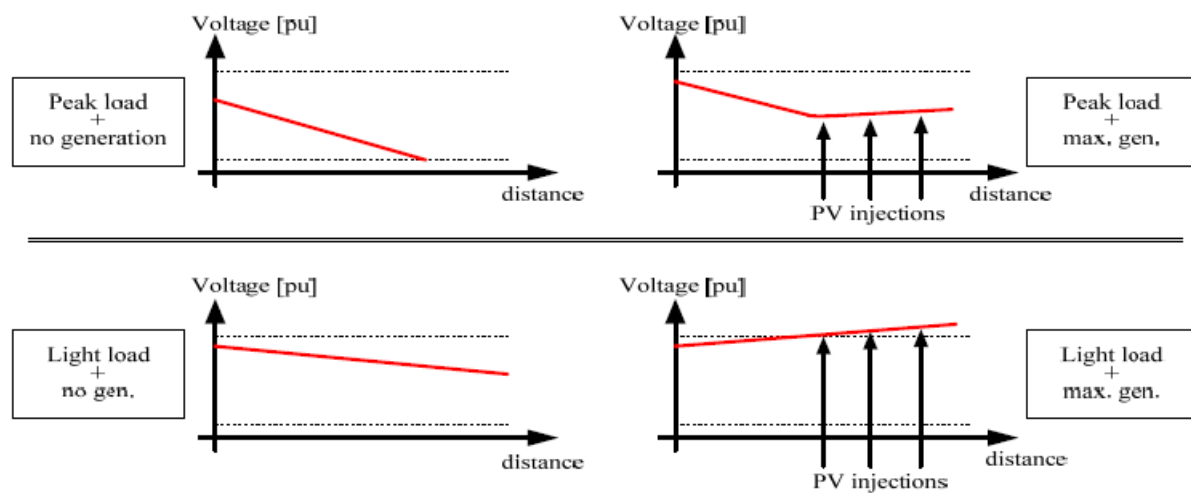


Figure 1-9 Challenged in Distribution Grids [7]

Further problems encountered in distribution grids are:

- Voltage rise = Mainly due to fluctuating power;
- Harmonics = Due to an increase of power electronics integrated in the grid;
- Flickers = Due to fluctuating power;
- Unbalances = Due to load demand not being even throughout the day.

Considering the above problems, grid codes need to be updated so that they can facilitate a secure and a reliable system.

Electricity in Denmark sits at a mediocre price comparing to the rest of Europe (including costs for cleaner energy), but because of the additional taxes, it makes it the highest electricity in Europe [17]. According to Energinet, the Transmission System Operator, the price for a kWh is approximately 2.1 DKK [4]. By 2015, the supply security in Denmark was over 99.99% being one of the highest in the world [18], explaining in some manner why the electricity price is so high.

The grid limits are presented in Table 1-1. Whereas electric vehicles are significantly heavy loads reaching up to 11 kW, the voltage dips may be extremely high. Thus, extra-precaution may be necessary, especially for the peak period (05:00 – 07:00 PM) when the consumers arrive home and plug-in their EV's.

Table 1-1 Power Quality Requirements [19]

Parameter	Supply Voltage	Limit
Frequency	LV-MV (50 Hz)	±1%
Voltage Magnitude	LV-MV	±10%
Supply Voltage Dips	LV	10-50%
	MV	10-15%
Short interruptions of supply voltage	LV-MV (up to 3 minutes)	10-900 times per year
Long Interruptions of supply voltage	LV-MV (more than 3 minutes)	48h/year
Harmonics	LV	THD≤8% (for each harmonic)
	MV	THD≤5% (for each harmonic)

1.3 Danish Smart Grid

As previously stated, the electrical consumption is expected to increase in a rapid manner. The consequences of this change will have an impact on the power quality, on grid losses and also voltage profiles will be changed considerably. In order to ameliorate these changes, Denmark when the concept of Smart Grid (Figure 1-10)

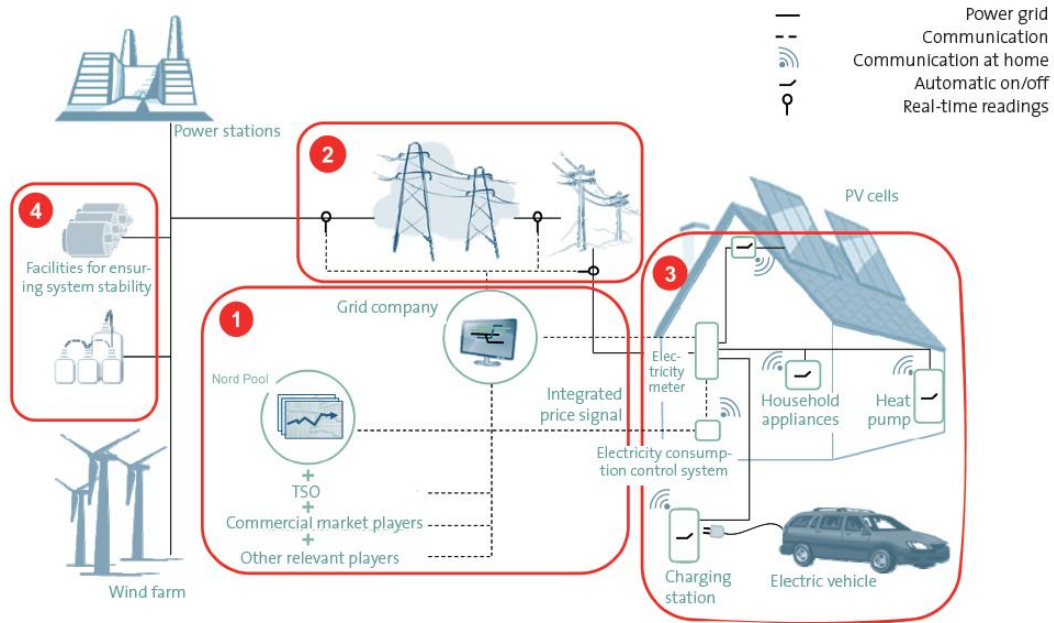


Figure 1-10 Illustration of the Elements of a Danish Smart Grid [20]

The objective is to make interactions between all the elements. As it can be seen in the figure above, wind farm, PV panels, electric vehicle, heat pump and the others interact to reduce the stress in the distribution grids, and also making the prices more economical for the consumers. Consumers may participate in regulating the market, by charging their EVs in the night when the electricity prices are lower [20]

Some of the most important concerns that are in a smart grid are:

- Frequency, which can be controlled by matching the generation and the consumption, assuring that every customer gets the electricity at the same frequency (50 Hz), with maximum 1% deviation as seen in Table 1-1.
- Voltage, especially voltage dips, which can be controlled by the usage of generators and transformers, also with special equipment like STATCOMs.
- Current, that has to be maintained between certain levels in order not to exceed the upper limit of the cables, consequently creating heating problems which translates into losses.

1.4 Electricity market in Denmark

Originally, the electricity market, like any other market, is divided into a wholesale market and a retail market. The main players that participate in trading are the producers, the retailers and the end users. Nevertheless, the electricity market trading system is more complex, new players such as, traders and brokers, enter the scene (Figure 1-11) [21]

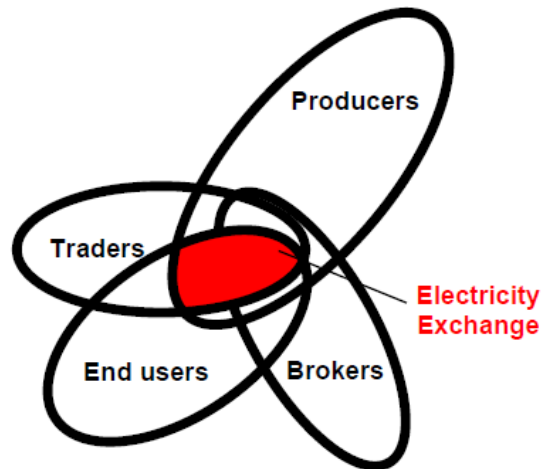


Figure 1-11 The commercial players and the electricity exchange [21]

Each player has its own role in the electricity market. In the trading process, the electricity is owned by the player, being able to buy the electricity from a producer and sell it to a retailer or to buy it from a retailer and sell it to another retailer. The broker acts as an intermediate in the trading process. For example, a broker may help a retailer to find a suitable producer who will sell an amount of electricity, at some time. Nord Pool Spot is an example of Nordic electricity market, which covers countries like Denmark, Norway, Sweden, Finland and Estonia [21]

1.4.1.1 The transmission system operator (TSO)

The role of the TSO is to keep the grid electrically stable in a particular area, keeping the frequency at 50 Hz and also to make sure that the end users receive the electricity. In Denmark, the TSO is the state-owned company called Energinet.dk [21]

1.4.2 Regulating power market

When consumption exceeds production, the frequency falls below 50 Hz and it surpasses 50 Hz in the other situation, therefore the system becomes unstable. As mentioned before, the TSO has the responsibility to correct these unbalances in the system, by making the producers to increase

or decrease the production. These processes are called „up-regulation”, respectively „down-regulation” [21]

1.4.3 Balancing Power

The electricity market transactions are made hourly. The figure below shows an example where the electricity is traded for one particular hour, called the hour of operation. The purchase must be made before the hour of operation.

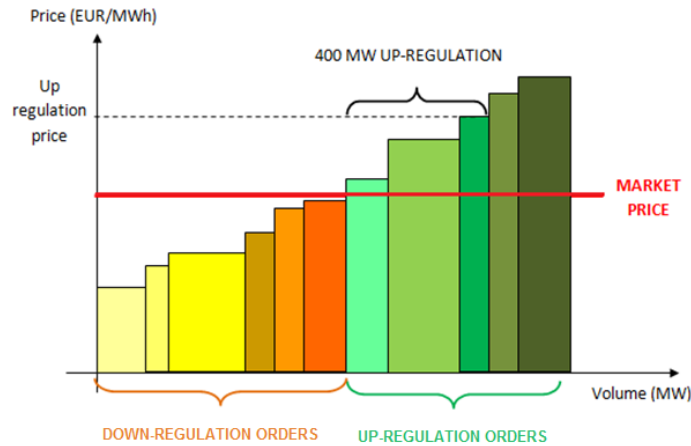


Figure 1-12 Price setting in the regulating power market [21]

1.4.4 Elspot – Nord Pool Spot’s Day-ahead Auction Market

Elspot market is the Nord Pool Spot’s day-ahead auction market. In this market, the power purchase orders or sell offers must be sent no later than noon the day before the power is supplied to the system. The market electricity price for a particular hour is set by intersecting the purchase curve with the demand curve (Figure 1-13). As both the buyers and the sellers have submitted orders, the price calculation in this market is called „double auction” .

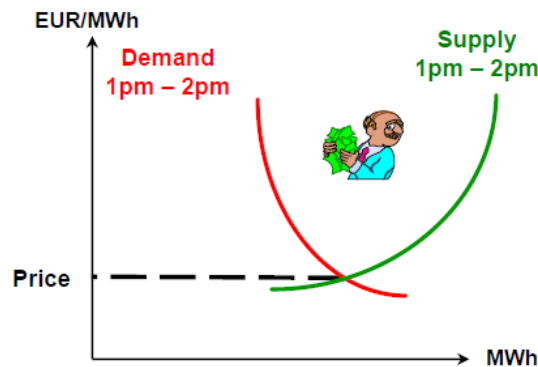


Figure 1-13 Supply Demand per one day [21]

1.5 Project Objectives

The main objective of this project is to conduct a technical analysis regarding the integration of renewable energy, heat pumps and electric vehicles in a distribution network. The goal is to find the maximum possible renewable generation for different scenarios of the system, as well as different control methods. Furthermore, an optimization method is analyzed for different charging strategies for electric vehicles.

The focus on renewable generation in Denmark is one of the highest in the world and it is expected to increase even more. Relying this much on renewable generation may cause improbabilities in generation.

The cold climate of Denmark, as a Nordic country, makes possible the need of heat pumps most of the year, exception in the summer, where temperature rises towards 20-30 degrees Celsius. Heat pumps are a great cheap environmental solution, as explained in 1.1.4.

Another solution for a cleaner environment is the electric vehicles, which are gaining increasingly interest. Electric vehicles not only that are environmental friendly, but they also help at integrating more renewable power as stated in 1.1.3, mainly due to their sizable load which depends on the type of vehicle (3-11 kW).

The power variations caused by renewables may sometimes challenge the system. The problems that may appear are presented in 1.2.

The project aims to identify and solve the problems caused by the high penetration of wind, solar power, using active and reactive power control, according to the grid codes. Further, an economic analysis regarding charging strategies of EVs will be analyzed.

In order to do this, the following objectives are considered:

- Modelling of renewable generation (wind and solar) and identify the maximum power supported by the grid;
- Modelling of the load side (heat pumps and electric vehicles), analyze how will they affect the system, and determine the new maximum renewable generation that can be integrated in the system;
- Analyze and compare active power control and reactive power control regarding the maximum renewable generation;
- Evaluate the impact of different charging strategies for electric vehicles technically as well as economically.

As mentioned in 1.1, wind and solar power generation are the top two renewable resources in Denmark, and will continue to be according to the experts' predictions. For this reason, the two

renewable generations are chosen to be studied in this project. On the other hand, due to the high penetration of renewables, EVs and heat pumps are integrated to balance the grid by consuming the extra generation. For this analysis to be more accurate, two periods of the year are chosen due to their differences in wind/solar production, January – high wind, low solar power production and July – low wind, high solar power production.

With big variations in the power production, it may cause voltage problems, transformer congestions and line loading problems. The main objective of the project is to determine the maximum allowable amount of wind power and PV production as well as EVs charging on a typical distribution grid with the help of active and reactive power control, while respecting all the problems mentioned previously.

In addition, economic strategies will be made to optimize the energy cost for both aggregators and consumers, while maintaining stable the operation of the system.

1.6 Methodology

In this master thesis the main program that is used is DigSILENT PowerFactory. With the help of this program, the steady state analysis is performed. The Newton-Raphson calculation method is used for load flow simulations. The control and optimization are made by using both Matlab and DPL, which is the programming language of DigSILENT.

The power curves of heat pumps and wind turbines is calculated in Matlab/Simulink. The optimization is based on the economical part of different charging schedules for the EVs.

Furthermore, Matlab is used to plot and analyze the output data from DigSILENT.

The described methodology is presented in steps as it follows:

- First, the validation of the IEEE 13 bus is made in order to have a common ground for all the upcoming scenarios, in winter/summer cases.
- Secondly, the grid is tested to see the maximum allowable wind/solar power it can support. Moreover, EVs and heat pumps are added to balance the system. Both cases are economically compared.
- For the charging of EVs, the first case is considered dumb charging (charging as soon as the consumer arrives home). To be a realistic case, the household consumption of Danish houses, the driving patterns and the available charging times are analyzed.
- Active and reactive power control of the system just for the WT, due to the bigger impact of wind speed in Denmark, and they are performed according to the grid codes.

- Furthermore, a smart charging strategy of the electric vehicles, the improvement of the system is analyzed from a technical and economical point of view.

1.7 Limitations

The limitations encountered in this project are:

- In this project, the study is limited to a relatively small residential distribution grid, and for this reason the wind speed and solar irradiation are considered equal for all wind turbines and solar photovoltaic panels.
- The load profiles are taken for one day in January, representing a higher base household consumption with more wind and lesser solar power, and one day in July, with slightly lower base household consumption, and with more solar power and lesser wind power generation.
- The wind turbines and photovoltaic panels are modelled as only active power generators (power factor of 1), except the reactive power control which will have variable power factor for the wind turbines. The heat pumps are modelled as loads with a power factor of 0.97, and the households are modelled with a power factor of 0.95. No heavy industry which would have a lower power factor is represented in this simulation.
- The study is performed on IEEE 13 bus network and not on a real network, and it is simulated with the fundamental frequency of 50 Hz (study is made for Denmark), different to the original model which is modelled with 60 Hz, as the model originates from America.
- The problems regarding the grid, such as voltage dips, flickering, harmonics are not considered.
- The analysis of heat pump integration is studied only in January case due to temperatures, in July being more or equal to the desired temperature (household temperature) which in this project is set to 20° C.
- The control methods are conducted with regards to the wind turbine power only.

1.8 Outline of the thesis

Chapter 1 – Introduction-In this chapter the background, project objectives, methodology of project, and project limitations, are studied for various components of the system.

Chapter 2 – Description of the distribution system – In order for the simulation to be as correct as possible, the need of validation occurs. In this chapter the validation of the IEEE 13 Bus Network is presented.

Chapter 3- Renewable Generation- For the simulation to be accurately performed, the profiles of each component should be accurately modelled. In this chapter the WT, PV , HP, EV are being modelled.

Chapter 4 – Maximum Allowable Renewable Integration with and without Heat Pump Integration. Having the validation completed, the study of the maximum renewable integration is performed. The impact of heat pumps is also analyzed with regards to the increase of renewable generation.

Chapter 5 – Control Schemes- In this chapter, the maximum renewable generation, discovered in chapter 4, is increased even more by performing active and reactive power control.

Chapter 6 – Economical Analysis- This chapter consists, of the techno-economic analysis, of different charging methods. The profits for the EV owners is determined, for both January and July.

Chapter 7- Conclusions and Future Work – In this chapter the conclusions determined by performing this analysis are shown. Further, future improvements to the study are shown.

2 Description and validation of the system

In this section, the IEEE 13 bus distribution system is presented and validated. Firstly, the process of power flow analysis is described, followed by the system description and finally, the validation of the model.

2.1 Power Flow Analysis

The power system flow analysis is a computational procedure which uses numerical algorithms to determine the steady state operating characteristics of a power system network from the given line and bus data [22]

As shown in Figure 2-1, the input for the load flow, consists of the line data and bus data the magnitude of bus voltage ($|V|$), and the angle of bus voltage referred to a common reference (δ) [22]

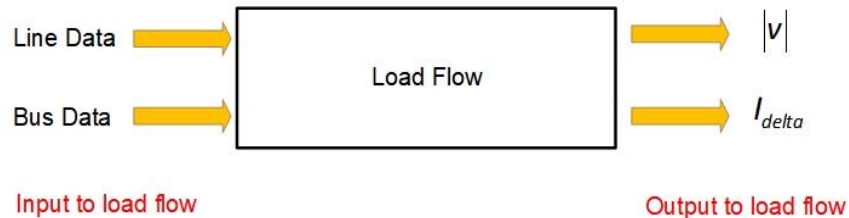


Figure 2-1 Load Flow Parameters

This method is used in power systems (transmission and distribution) in order to have a fast analysis of the current state of the system. The speed of the steady state analysis is highly important, some simplified component models are used, as shown in Table 2-1.

Table 2-1 Simplified Models for Electrical Equipment [19]

Equipment	Simplified Model
Short Lines (below 80 km)	Series Impedance
Medium and Long Lines (above 80 km)	π model
Transformer	Series Reactance
Loads	Constant Power
Generators	Constant power source operating at a fixed voltage

In Figure 2-2 the transmission line model (π model) is presented. It is modelled on the bases of the π model, where $R + jX$ is the line impedance, and $Y/2$ is the half line charging admittance.

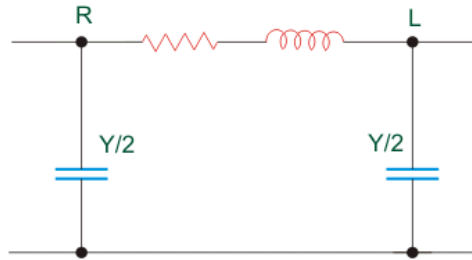


Figure 2-2 Transmission Line Model

In each load flow study, the type of each bus bar is divided in three types. Each of these types is different, each having its role into performing the load flow analysis.

In each power flow study, there are three types of buses, which are determined by the known and unknown variables. Depending on which components are present in the system and on the known variables, the type of bus can be determined.

2.1.1 Voltage Controlled Bus

The model of the PV bus or Voltage controlled bus, where the generation is connected, is presented in Figure 2-3. The value of the voltage magnitude is maintained at a constant level for as long as the reactive power is maintained between the limits ($Q_{\min} < Q_{\text{required}} < Q_{\max}$). If the reactive power gets over the limits, the bus becomes a load bus (PQ bus) with the Q limit that has been breached, as the new reactive power for the bus. Equation (1) describes the total generation power at node “i”. [22]

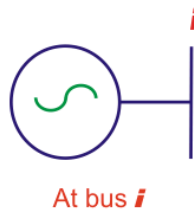


Figure 2-3 PV Bus

$$S_{Gi} = P_{Gi} + jQ_{Gi} \quad (1)$$

2.1.2 PQ Bus (Load Bus)

The model of PQ bus, also known as a load bus, is depicted in Figure 2-4. In a power system this type of buses represent 85% of the total number of nodes. The total power demand is presented in equation 2 [22]

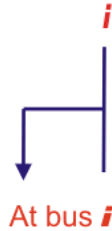


Figure 2-4 Load Bus Model

$$S_{D_i} = P_{D_i} + jQ_{D_i} \quad (2)$$

2.1.3 Slack Bus

The slack bus, also known as the reference bus, is limited to just one in every system. The phase angles of all the other buses are relative to the slack bus angle. In real life, the slack bus doesn't exist, it is used just for simulations. All the losses in the system that are not supported by other types of generators are supported by the slack bus. Another important feature is that the slack bus has to adjust the power to hold the voltage constant [22]

Table 2-2 Bus Types Specified vs Unspecified parameters presents the specified and unknown variables for the load flow for all 3 types of buses.

Table 2-2 Bus Types Specified vs Unspecified parameters [22]

Bus Type	Specified Variables	Unknown Variables
PQ	P, Q	V , δ
PV Bus	P, V	Q, δ
Slack Bus	V , δ	P, Q

2.1.4 The Bus Admittance Matrix

The bus admittance matrix or the node admittance matrix is used in energy engineering to describe a power system with N buses, which is a square matrix composed of N by N elements. This matrix is used to calculate all the parameters necessary such as voltages or angles for each node [50].

In Figure 2-5 it is presented a simple 4-bus network with 2 generation nodes and a transformer.

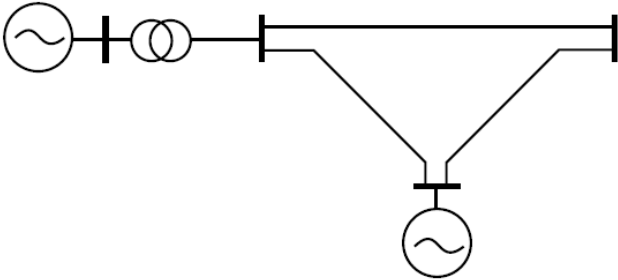


Figure 2-5 Simple 4 Bus Network

Considering the 4-bus network, it can be easily understood how the unknown variables can be represented, knowing just two variables for each bus, using Table 2-2 [22]

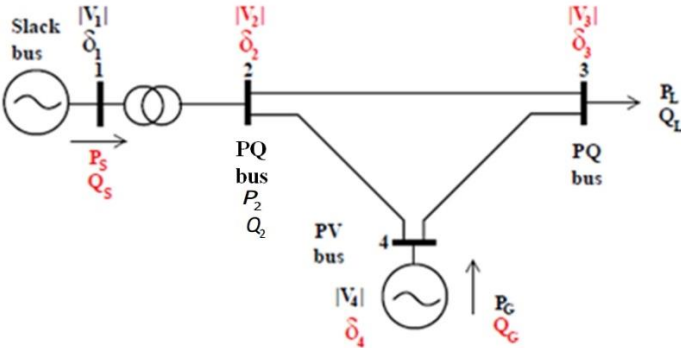


Figure 2-6 Simple 4 Bus Network with variables [19]

Moreover, the normal network presented in Figure 2-5 needs to be transformed into a bus admittance diagram. In Figure 2-7, it is presented the bus admittance diagram of the system represented in Figure 2-5.

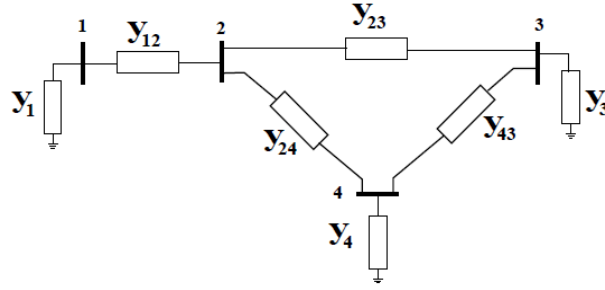


Figure 2-7 Bus Admittance Diagram

Further, the admittance elements y_{ij} are calculated for each point of the diagram. The formula is presented in equation 3:

$$y_{ij} = \frac{1}{Z_{ij}} = \frac{1}{R_{ij} + jX_{ij}} \quad (3)$$

Where, y_{ij} [$\text{I}\Omega^{-1}\text{I}$] is the admittance between nodes i and j ; z_{ij} is the impedance from node i and j ; r_{ij} [Ω] is the resistance part, and x_{ij} [Ω] is the reactance between nodes i and j .

After the admittances for all the buses (y_{ij}, y_{ii}) have been calculated, the next step is to calculate the mutual admittances, that will be used to build the admittance matrix. The equation is presented in (3):

$$Y_{ij} = -y_{ij} \quad (3)$$

Furthermore, the self-admittance elements for each node must be calculated. They are equal to the sum of admittances connected to that particular node. The position for each element will be on the diagonal axis of the bus admittance matrix, and it can be calculated using equation (5):

$$Y_{ii} = y_{ij} + \sum_{\substack{n=1 \\ n \neq i}}^N y_{in} \quad (4)$$

After all the necessary elements have been calculated, the admittance matrix can be built. For the system presented in Figure 2-6, the admittance matrix is shown below:

$$Y_{nn} = \begin{bmatrix} Y_{11} & Y_{12} & Y_{13} & Y_{14} \\ Y_{21} & Y_{22} & Y_{23} & Y_{24} \\ Y_{31} & Y_{32} & Y_{33} & Y_{34} \\ Y_{41} & Y_{42} & Y_{43} & Y_{44} \end{bmatrix} \quad (5)$$

One big advantage of the Y_{bus} is that it has symmetric elements along the diagonal axis, meaning that $Y_{12}=Y_{21}$, $Y_{13}=Y_{31}$ and so on. Furthermore, in a power system not all the nodes are connected together, making the bus admittance matrix a sparse matrix with many elements being 0. This reduces significantly the computational time and the required storage [23]

As shown in Table 2-2 Bus Types Specified vs Unspecified parameters [22], there are different types of buses, with different specified variables and unknown variables. By knowing what type of bus is, there can be calculated the active and reactive power of the node, with the help of power flow equations shown below:

$$P_k = \sum_{j=1}^N |V_k| |V_j| (G_{kj} \cos(\theta_k - \theta_j) + B_{kj} \sin(\theta_k - \theta_j)) \quad (6)$$

$$Q_k = \sum_{j=1}^N |V_k| |V_j| (G_{kj} \sin(\theta_k - \theta_j) + B_{kj} \cos(\theta_k - \theta_j)) \quad (7)$$

Where:

P_k =active power at node k; Q_k =reactive power at node k; V_k =voltage at node k; V_j =voltage at node j; G_{kj} =real component of the element in the admittance matrix between node k and j; B_{kj} =imaginary component of the element in the admittance matrix between node k and j; θ_k =voltage angle at node k; θ_j =voltage angle at node j.

For simple system networks, the power flow can be done manually using equations 7 and 8. For more complex network systems, iterative methods are used.

The most important methods are:

- Gauss-Siedel Method (G-S);
- Newton-Raphson Method (N-R);
- Fast Decoupled Method (FDLF).

A comparison between the three methods, where criteria such as system size, storage and more is presented in Table 2-3.

Table 2-3 Comparison between load flow methods.[24]

	G-S	N-R	FDLF
System size	Smaller	Unlimited	Unlimited
Storage	Minimal	Large	40% of N-R
Programming	Easy	Complex	Less complex
Convergence	Worst	Best	Good
Accuracy	Less	Most	Good

As it can be seen in the table above, Newton-Raphson convergence method has the best results. The only disadvantage is that the programming is complex. In Simulation programs such as DigSILENT PowerFactory, the Newton-Raphson method is used.

2.2 IEEE 13 bus distribution system validation

The validation of the IEEE 13 bus network system is needed in order to create a benchmark model of the distribution grid for the simulations which are performed on it. After the validation is performed, renewables, electric vehicles and heat pumps are added, and the system is tested, different scenarios and scenarios. In Figure 2-8, the IEEE 13 Bus test network is presented.[25]

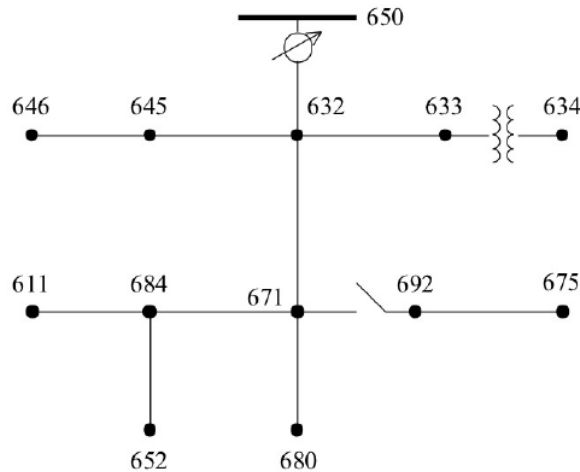


Figure 2-8 IEEE 13 Bus Test Network [25]

The distribution model [54], shown above, is modeled using DigSILENT Powerfactory, and it is presented in Figure 2-9 including just the base model, where the validation is performed.

Table 2-4 Voltage and Power Profiles for Phase A

NODE	Sim V_A (p.u.)	IEEE V_A (p.u.)	Diff (%)	Sim P_A (kW)	IEEE P_A (kW)	Diff (%)	Sim Q_A (kVAr)	IEEE Q_A (kVAr)	Diff (%)
RG60	1.05	1.05	0	-	-	-	-	-	-
632	1.0413	1.042	0.067	-	-	-	-	-	-
645	1.0317	1.0329	0.116	-	-	-	-	-	-
646	1.03	1.0311	0.1	-	-	-	-	-	-
633	1.0392	1.041	0.17	-	-	-	-	-	-
634	1.02	1.0218	0.176	160	160	0	110	110	0
671	1.0531	1.0529	0.1	390	385	1.3	219.3	220	0.4
684	-	-	-	-	-	-	-	-	-
611	-	-	-	-	-	-	-	-	-
692	1.0531	1.0529	0.1	-	-	-	-	-	-
675	1.0551	1.0553	0.018	470	485	3.1	190	190	0
680	1.0531	1.0529	0.1	-	-	-	-	-	-
652	-	-	-	120	123.56	2.9	80	83.02	3.7

Table 2-5 Voltage and Power Profiles for Phase B

NODE	Sim V_B (p.u.)	IEE V_B (p.u.)	Diff (%)	Sim P_B (kW)	IEE P_B (kW)	Diff (%)	Sim Q_B (kVAr)	IEEE Q_B (kVAr)	Diff (%)
RG60	1.05	1.05	0	-	-	-	-	-	-
632	1.0413	1.042	0.067	-	-	-	-	-	-
645	1.0317	1.0329	0.116	175.6	170	-	130	125	-
646	1.03	1.0311	0.1	242.1	240.66	-	136.5	138.12	-
633	1.0392	1.041	0.17	-	-	-	-	-	-
634	1.02	1.0218	0.176	120	120	0	90	90	0
671	1.0531	1.0529	0.1	405.1	385	5.1	218	220	0.2
684	-	-	-	-	-	-	-	-	-
611	-	-	-	-	-	-	-	-	-

692	1.0531	1.0529	0.1	-	-	-	-	-	-
675	1.0551	1.0553	0.018	73.2	68	3.1	68	60	3.8
680	1.0531	1.0529	0.1	-	-	-	-	-	-
652	-	-	-	-	-	-	-	-	-

Table 2-6 Voltage and Power Profile for Phase C

NODE	Sim V_C (p.u.)	IEEE V_C (p.u.)	Diff (%)	Sim P_C (kW)	IEEE P_C (kW)	Diff (%)	Sim Q_C (kVAr)	IEEE Q_C (kVAr)	Diff (%)
RG60	1.05	1.05	0	-	-	-	-	-	-
632	1.0413	1.042	0.067	-	-	-	-	-	-
645	1.0317	1.0329	0.116	-	-	-	-	-	-
646	1.03	1.0311	0.1	-	-	-	-	-	-
633	1.0392	1.041	0.17	-	-	-	-	-	-
634	1.02	1.0218	0.176	120	120	0	90	90	0
671	1.0531	1.0529	0.1	370	385	3.9	220	220	0
684	-	-	-	-	-	-	-	-	-
611	-	-	-	160	165.54	3.4	74.3	77.9	4.6
692	1.0531	1.0529	0.1	171.3	168.37	1.71	146.9	149.55	1.77
675	1.0551	1.0553	0.018	270	290	5.89	200	212	5.6
680	1.0531	1.0529	0.1	-	-	-	-	-	-
652	-	-	-	-	-	-	-	-	-

2.3 Summary

After analyzing the tables mentioned above, it can be concluded that the highest differences are for phase C for node 675. Here for active and reactive power the difference is 5.89 % and 5.6 %, respectively. The difference for the reactive power can be explained by mentioning that the IEEE 13 bus network originates from America, where the nominal frequency is 60 Hz, not valid in Europe. The simulations of the model with 50 Hz changes the reactance, as well as the reactive power.

Because all the results are close to/below the 5% difference margin, it can be concluded that the model is validated with respect to the IEEE 13 bus network model [52]. Therefore, the validated model will be used for further investigations where maximum renewable energy is tested in combination with electric vehicles and heat pumps. For the upcoming simulations, the voltage regulators (phase A, phase B, phase C) are replaced by a 3-phase transformer since there will be no more unbalances in the loads, everything being 3-phase.

3 Modelling of the generation and consumption profiles

As shown in List of Figures

Figure 1-1 Installed RE Capacity in Europe [MW] 2000-20016 [3].....	11
Figure 1-2 Installed Wind Capacity in Denmark [3]	11
Figure 1-3 Wind Turbines by Capacity in Denmark [4].....	12
Figure 1-4 Installed Capacity of Photovoltaic Panels in Denmark [3]	13
Figure 1-5 Number of PVs in Denmark [4]	13
Figure 1-6 Comparison of the costs of ownership of EVs compared to Petrol and Diesel Vehicles [10].....	16
Figure 1-7 Expected Future EV share [8]	16
Figure 1-8 Heat Pump Cycle [14].....	17
Figure 1-9 Challenged in Distribution Grids [7].....	18
Figure 1-10 Illustration of the Elements of a Danish Smart Grid [20]	20
Figure 1-11 The commercial players and the electricity exchange [21].....	21
Figure 1-12 Price setting in the regulating power market [21].....	22
Figure 1-13 Supply Demand per one day [21].....	22
Figure 2-1 Load Flow Parameters.....	27
Figure 2-2 Transmission Line Model	28
Figure 2-3 PV Bus	28
Figure 2-4 Load Bus Model.....	29
Figure 2-5 Simple 4 Bus Network	30
Figure 2-6 Simple 4 Bus Network with variables [19]	30
Figure 2-7 Bus Admittance Diagram.....	31
Figure 2-8 IEEE 13 Bus Test Network [25]	33
Figure 2-9 DigSilent PowerFactory 13 Bus Network.....	34
Figure 3-1 Wind power generation and household electricity consumption for January and July.....	41
Figure 3-2 Wind Speed vs Power Curve for Osiris 10 turbine	42
Figure 3-3 Wind Speed and Wind Power Generation for 1 day in January/July.....	43
Figure 3-4 PV Power Generation July and January.....	47
Figure 3-5 The Lift [59]	48
Figure 3-6 COP vs Lift [30].....	48
Figure 3-7 Thermal Energy vs Electrical Energy	49
Figure 3-8 Average daily driving distance in DK [32]	50

Figure 4-1 The Critical Components of the system	53
Figure 4-2 Household Electricity Consumption January/July 2013.....	55
Figure 4-3 Max Renewable Cases 1-4 January.....	57
Figure 4-4 Node 675 Voltage Levels January	58
Figure 4-5 Transformer Loading January	58
Figure 4-6 Line Loading January Case	59
Figure 4-7 Max Renewable Generation (WT+PV) January	60
Figure 4-8 Maximum Renewable integration July	61
Figure 4-9 Transformer Loading in July.....	62
Figure 4-10 Node 675 Voltage in July.....	63
Figure 4-11 Lines Loading July	64
Figure 4-12 Renewable Maximum Generation July	64
Figure 4-13 New Maximum Renewable Generation January.....	65
Figure 4-14 Old vs New Generation January	66
Figure 5-1 Active Power Control Flowchart.....	69
Figure 5-2 Max WT January.....	70
Figure 5-3 Voltage, Transformer and Line profiles for 850 WTs (January)	71
Figure 5-4 Max WT July (600 WTs)	72
Figure 5-5 Voltage, Transformer and Main Line profiles for 600 WTs (July).....	73
Figure 5-6 Reactive Power Control profiles (January)	75
Figure 5-7 Reactive Power Control (July)	76
Figure 6-1 Simulation Method of EV Charging	79
Figure 6-2 Dumb Charging January	81
Figure 6-3 Loading difference between the Main and Second Transformer	82
Figure 6-4 Smart Charging Profiles	84
Figure 6-5 Dumb charging profiles- July.....	86

Summary

Renewable Generation such as Wind Power Generation as well as Solar Power Generation, is on a continual rise. Relying this much on renewable integration, may stress the system, and also generate unbalances in the system. Methods to store the extra energy when the production is bigger than consumption (especially in the night). Loads such as Electric Vehicles and Heat Pumps.

In this master thesis, the renewable integration is modelled and raised to the maximum capability that the system can support, regarding its limits. The system is modelled and validated on the IEEE 13 Bus Network. Furthermore, Heat pumps are integrated as well into the system, in order to increase the consumption, during the off-peak household consumption hours. After the integration of heat pumps, the number of wind turbines possible to operate in the system, increases by 10 times.

Control Methods are further analyzed, to increase even more the renewable generation that can be integrated into the system. Active Power Control consists of lowering the power production in the periods where the system limits may be violated.

Another type of control, analyzed in this project, is the reactive power control, based on generating or consuming reactive power in order to keep the system in its established limits. By doing this method, the maximum number of Wind Turbines and PV panels are found.

Finally, different charging strategies are studied, in order to find the highest profit for the EV owners, while keeping the system under the limits.

Introduction, the number of PV installments in Denmark has abruptly increased over the last years and it will continue to rise. Furthermore, wind turbines are widely used due to the high winds available here.

In this chapter, the solar, wind, heat pumps and EVs power curves are presented by showing the models which were used to determine the generated (WT and PV) or consumed (EV and HP) power.

For this project, the data used to calculate the renewable generation power curves (WT+PV) is based on [26], recorded in Aalborg, Denmark, for one year, from 01/01/2013 - 31/12/2013.

Two periods of the year, January and July, have been considered for further studies. These months are representative for the higher consumption in January (Winter case) due to the heating and lightening, and also high wind speeds. On the other hand, July has periods with the lowest consumption in the year and lower wind speeds, but much more solar power. Furthermore, as the wind is the most important renewable energy source in Denmark, a 2-week (17-01-2013 to 31-01-2013 and 17-07-2013 to 31-07-2013) visualization profile is conducted in Figure 3-1 in order to better understand the behavior of both wind production and consumption, for both periods. In the figure below, it can be seen that on average, the wind power production is higher in January, compared to July. For further analysis, 28-01-2013 and 26-07-2013 have been chosen, as their wind power profiles are neither too low or too high.

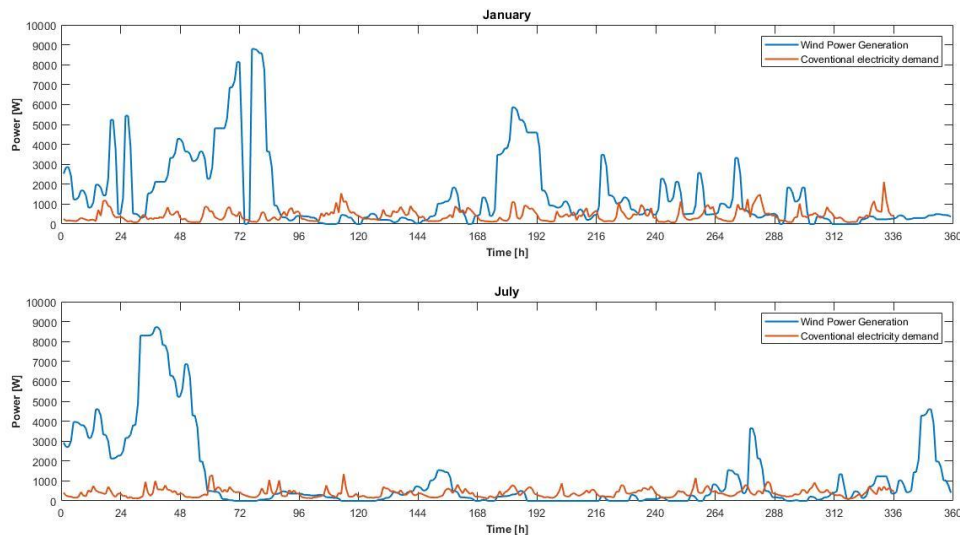


Figure 3-1 Wind power generation and household electricity consumption for January and July

3.1 Wind Turbines Power Simulation

For the wind turbine generation case, the power is determined using a look-up table in Matlab/Simulink, where the input is the wind speed and the output is the power generated. The lookup table consists of a Wind vs Power curve (v-P) for the Osiris 10, 10 kW wind turbine. This turbine is accepted in the Danish Market, according to [27]. The control of the power is done with the help of the active and passive pitch control [27]. Some important specifications of the turbine are shown below in Table 3-1.

Table 3-1 Osiris 10 Wind Turbine Specifications [28]

Specifications	Values
Rated Power	10 kW
Cut in Wind Speed	2.5 m/s
Cut out Wind Speed	22 m/s
Rated Wind Speed	9.5 m/s
Passive Power Regulation	Pitch angle adjustment
Blade Diameter	9.7 m

Furthermore, the wind speed – power curve used in the look-up table is shown in Wind Speed vs Power Curve for Osiris 10 turbine.

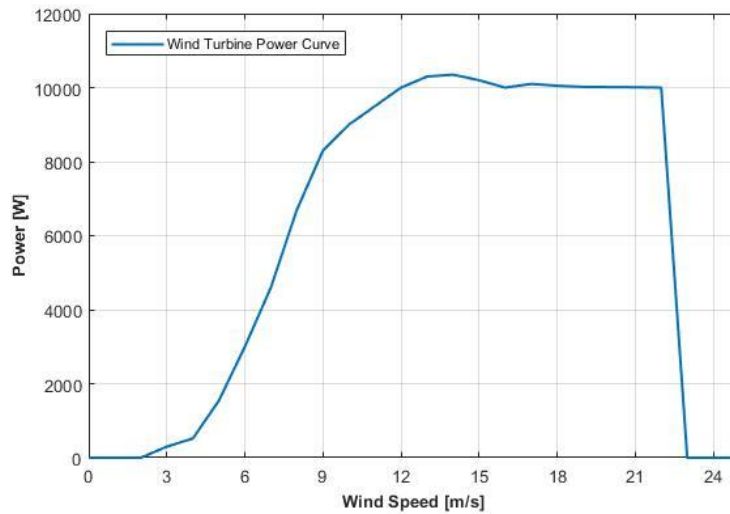


Figure 3-2 Wind Speed vs Power Curve for Osiris 10 turbine

In Figure 3-3, the wind speed for a day in January and a day in July, as well as the power generated by one wind turbine with the wind speed, are presented. During winter the wind is more significant throughout the day, than during the night. Consequently, the power of the wind turbines provided will be as well higher. For July, the power is almost zero until 12 AM, due to the restriction of the turbine cut-in wind speed.

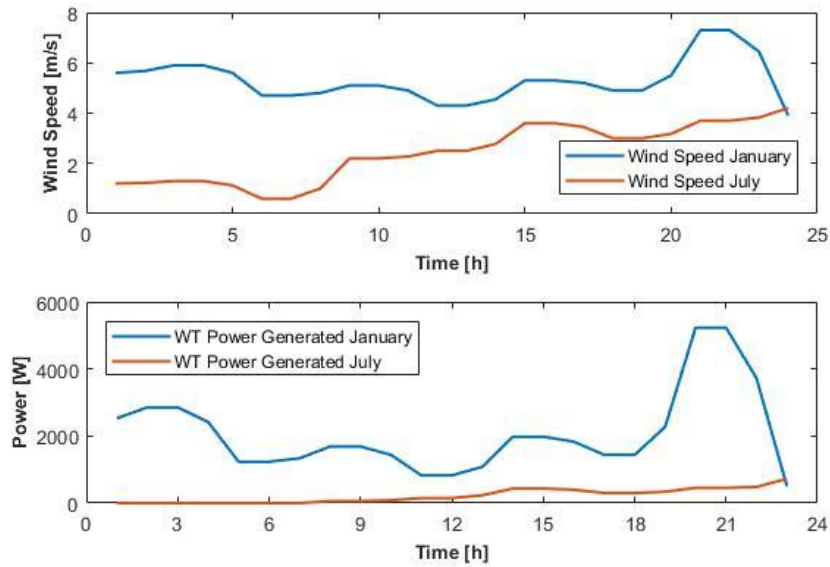


Figure 3-3 Wind Speed and Wind Power Generation for 1 day in January/July

3.2 Photovoltaic Panels Power Simulation

The PV system comprises 6 panels, with a rated power of 225 W each panel, resulting a total rated a power of 1350 W.

For the Power Curve Simulation of the PV panels the following parameters were taken from [26]:

- Global Horizontal Irradiance (G)
- Diffused Horizontal Irradiance (Gd)
- Solar Azimuth Angle (AZ)
- Air Temperature (Ta)

Considering 4 parameters instead of one, as in the case of Wind Power Simulation subchapter, a more thorough calculation is needed to perform in order to accurately calculate the power curve. Furthermore, taking into consideration these parameters, one can find the output power of the PV in three steps. Firstly, the total tilted irradiance is calculated, using the Perez irradiance model [4]. This is done with respect to the tilted angle of the PVs used in Denmark, which is 42° [2]. Secondly, The PV cell temperature is calculated, because the output power is dependent on the air temperature. The air temperature is desired to be as low as possible for a better efficiency of the PV panel. Finally, the PV power is calculated, with respect to the area of the PV panels, which in this case were taken to be 4 PV panels summing up an area of 6.4 m^2 .

3.2.1 Total tilted irradiance calculation

The total tilted irradiance ($G_{total-tilted}$) has been calculated for one year from the provided data using the Perez irradiance model. To calculate $G_{total-tilted}$ the following calculations have been conducted.

The direct horizontal irradiance (G_b) is calculated using the equation below:

$$G_b = G - G_d \quad (8)$$

The zenith angle (ZA) and the incidence angle (IA) are calculated using the following equations:

$$ZA = 90^\circ - SA \quad (9)$$

where SA is the solar altitude angle in degrees.

$$IA = \arccos[\cos(ZA) * \cos(\beta) + \sin(\beta) * \cos(AZ)] \quad (10)$$

where AZ is the solar azimuth angle, in degrees, and β is the tilt angle, considered 42° for Denmark, according to [5].

Further, the day angle (B), in radians, is calculated:

$$B = \frac{2\pi * (dn - 1)}{365} \quad (11)$$

where dn is the day number, for one year. And for this simulation dn=208 (July) and dn=28 (January).

The eccentricity correction factor of the earth's orbit (E_0) using the day angle (B) value for each day, is calculated:

$$E_0 = 1 + 0.034 \cos(B) + 0.001 \sin(B) + 0.0007 \cos(2B) + 0.00007 \sin(2B) \quad (12)$$

Next, E_0 is used to calculate the extraterrestrial irradiance on horizontal surface (G_{on}):

$$G_{on} = G_{sc} * E_0 \quad (13)$$

where $G_{sc} = 1367 \text{ W/m}^2$.

The relative optical air mass (m) is calculated below:

$$m = [\sin(SA) + 0.15(SA + 3.885)^{-1.253}]^{-1} \quad (14)$$

where SA is in degrees.

Further, the sky clearness (ϵ) is calculated:

$$\epsilon = \frac{(G_d + G_b)}{(G_d + 1.041ZA^3)} \quad (15)$$

where ZA is the zenith angle measured in radians, this time.

The irradiance coefficients are obtained from the table below, based on the value of ϵ .

Table 3-2 Irradiance Coefficients with respect to the Sky Clearness

ϵ	F_{11}	F_{12}	F_{13}	F_{21}	F_{22}	F_{23}
1	-0.008	0.588	-0.062	-0.060	0.072	-0.022
2	0.130	0.683	-0.151	-0.019	0.066	-0.029
3	0.330	0.487	-0.221	0.055	-0.064	-0.026
4	0.568	0.187	-0.295	0.109	-0.152	-0.014
5	0.873	-0.392	-0.362	0.226	-0.462	0.001
6	1.132	-1.237	-0.412	0.288	-0.823	0.056
7	1.060	-1.600	-0.359	0.264	-1.127	0.131
8	0.678	-0.327	-0.250	0.156	-1.377	0.251

Using the irradiance coefficients from the table above, the circumsolar (F_1) and horizon brightening coefficients (F_2) are calculated:

$$F_1 = F_{11} + F_{12}\Delta + F_{13}Z \quad (16)$$

$$F_2 = F_{21} + F_{22}\Delta + F_{23}Z \quad (17)$$

Where (Δ) is the sky's brightness and it can be calculated using the equation below:

$$\Delta = \frac{G * m}{G_d} \quad (18)$$

Further, the beam, tilted irradiance and the reflected irradiance are calculated:

$$G_b(\beta) = G_b * \frac{a}{b} \quad (19)$$

$$G_d(\beta) = G_d * \left((1 - F_1) \frac{(1 + \cos(\beta))}{2} + F_1 * \frac{a}{b} + F_2 * \sin(\beta) \right) \quad (20)$$

where: $a = \max(0, \cos(IA))$ and $b = \max(0.087, \cos(ZA))$

$$G_r(\beta) = G * pg * \frac{(1 - \cos(\beta))}{2} \quad (21)$$

where: $\beta=42^\circ$ and $pg=0.2$.

Finally, $G_{total-tilted}$ is given by equation:

$$G_{total-tilted} = G_b(\beta) + G_d(\beta) + G_r(\beta) \quad (22)$$

3.2.2 PV cell temperature calculation

The total tilted irradiance, calculated before, is now used to calculate the temperature of the PV:

$$T_c = T_{air} + \frac{NOCT - 20}{800} * G_{total-tilted} \quad (23)$$

where NOCT is the normal operating cell temperature and it is considered 45° .

PV output power calculation

Finally, the PV output power is calculated following the next steps:

$$\eta_{pv} = \eta_{ref} [1 - k_T (T_c - 25^\circ)] \quad (24)$$

where $\eta_{ref}=0.15$ is the reference solar cell efficiency and $k_T=0.004$ is the temperature coefficient.

$$P_{pv} = \eta_{pv} * G_{total-tilted} * A \quad (25)$$

where A is the PV module area, expressed in m^2 .

Finally, the power can be seen in Figure 3-4, shown below, for a day in July and one in January. As expected, the power generated in July is bigger than the one generated in January, due to more irradiance being available in July.

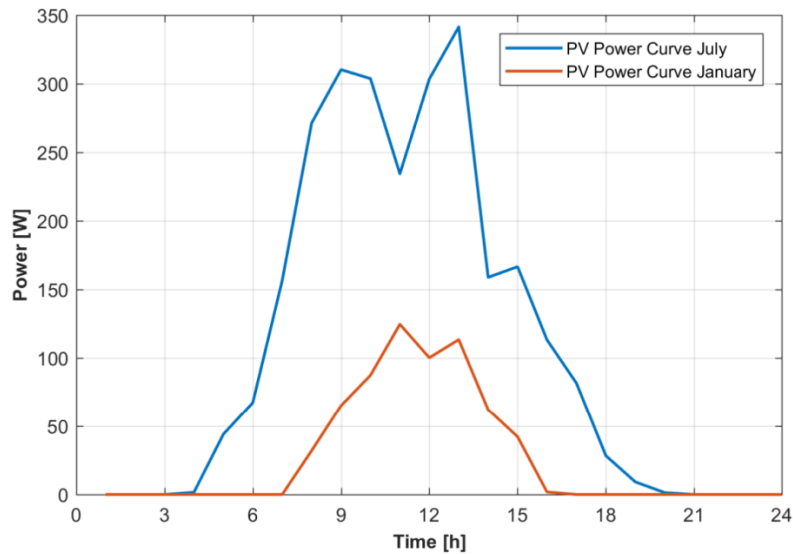


Figure 3-4 PV Power Generation July and January

3.3 Heat Pump Power Demand

As mentioned in chapter 1, heat pumps can act as a load, helping the system by storing the excess power. In this project the air-air heat pumps will be used as being the most common in Denmark.

Heat pumps efficiency is greatly depending on the operating temperatures. These temperatures are the outside temperature, called ‘source temperature’ (environmental temperature), from where the air is extracted. The temperature where the air is delivered is called ‘sink temperature’. The difference between the source temperature and the sink temperature is also known as ‘lift’. The smaller the lift is, the bigger the efficiency, due to the lesser energy needed to reach the desired temperature. For example, the energy needed to heat an apartment at 20 °C with the outside temperature of 2 °C, will be smaller than the energy needed to heat the apartment at the same temperature, with the outside temperature being -10 °C. [29]

In Figure 3-5 a better representation of the lift is presented, from an outside temperature of -20 °C to a desired temperature of 20°C.



Figure 3-5 The Lift [59]

Heat Pumps heating efficiency can be expressed with the help of the performance coefficient (COP). For heating purposes, COP can be expressed as the heat energy delivered by the heat pump divided by the energy needed from the pump, compressor, and the fan [29]

$$COP_{heating} = \frac{UsefulHeatingEnergy}{CompressorEnergy + FanEnergy + PumpEnergy} \quad (26)$$

Since the energy required by the heat pump (compressor, fan and pump) is less than the actual useful thermal energy provided by the heat pump, this coefficient (COP) will be always bigger than 1. For example, for a COP equal to 3, excluding the energy drawn from the environment calculations, a heat pump can provide 3 kWh thermal energy for heating with just 1 kWh electrical energy [29]

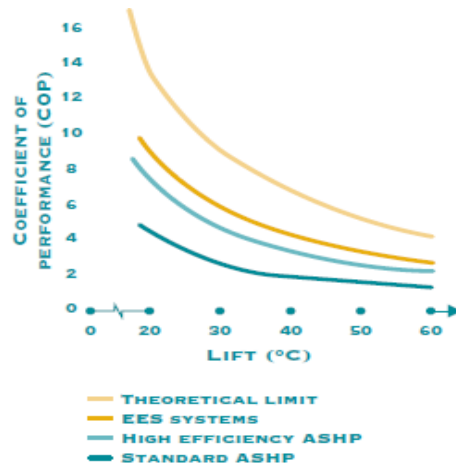


Figure 3-6 COP vs Lift [30]

In Figure 3-6, a graphical relation between COP and Lift is presented for different types of heat pumps. In this project, the most common Standard Air Sourced Heat Pump is utilized, which is the heat pump with the lowest COP [30]

Finally, in Figure 3-7 the electrical energy needed for one day in January for an air-air heat pump is shown. Between 00:00 -06:00 A.M., where the outside temperature is lower, it is seen that the thermal power provided is big in order to keep the temperature constant at 20 °C. Following the period of 12:00 to 06:00 P.M. no power is required due to the inside temperature keeping constant at the set temperature (20°C).

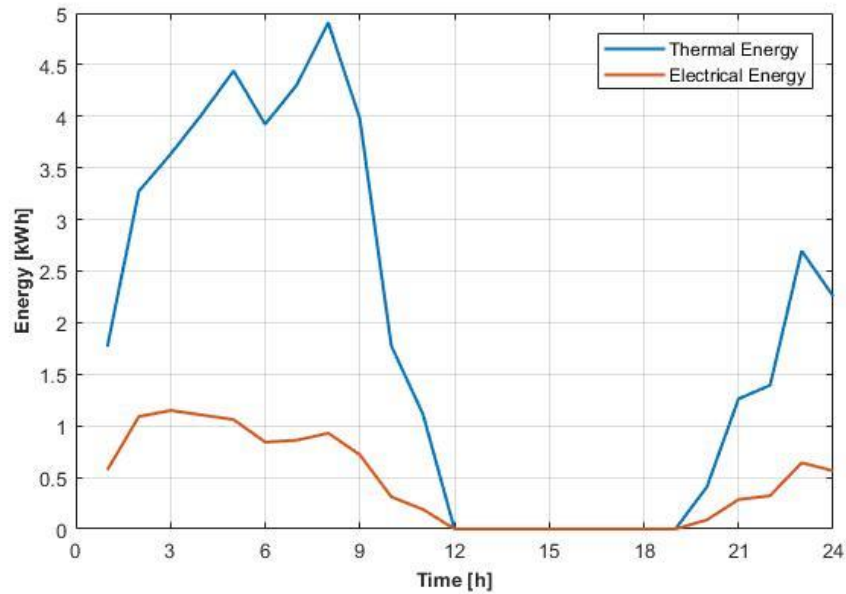


Figure 3-7 Thermal Energy vs Electrical Energy

According to the Danish Energy Agency [31] in 2014 the percentage of heating for Denmark just from heat pumps was approximately 12%. Since heat pump installations are on a continuing rise as stated in chapter 1, the percentage of heat pumps in the current project is set to 12%.

3.4 Electric Vehicle Integration

To accurately integrate electric vehicles into the simulation, some important parameters have to be taken in consideration, such as: percentage of EVs of the total vehicles, charging profiles, arriving times of EVs, consumption/km, distances travelled.

For the parameters, three data sources will be used in this project [30]

- MDCars (Database of Odometer readings);
- TU Data (Danish National Transport Survey);
- AKTA Data (GPS-Based Data that Follows the Vehicles).

These sources analyze the behavior of the EV owners and record the data in order to better predict certain aspects in the future.

3.4.1 Number of EVs

As presented in section Electric Vehiclesthe estimated number of EVs in Denmark is 20% of the total vehicles. For this project, it is assumed that for all houses (6405 total) 20% of them have an electric vehicle.

3.4.2 Driving Distance

The average driving distance for each day of the week is presented in Figure 3-8 The highest distance travelled is 55 km in a Friday. For this project, the overall distance is taken as the average distance of all days, 48 km [32]

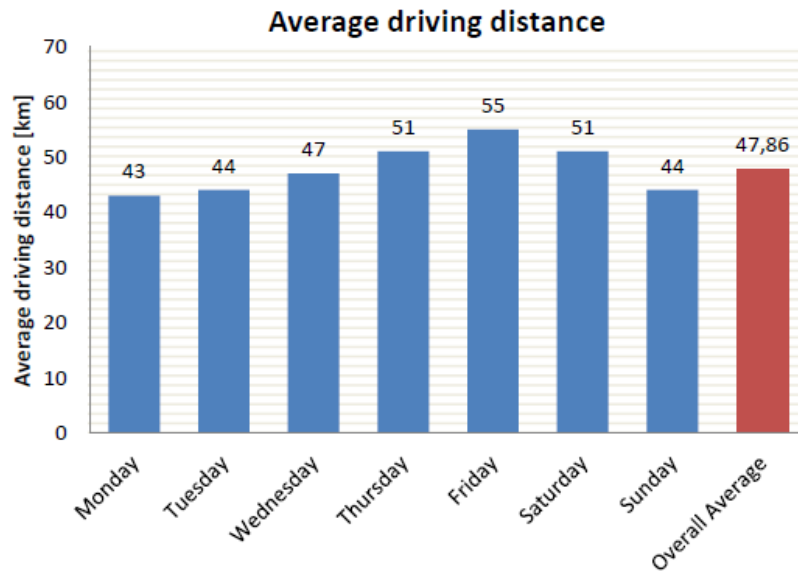


Figure 3-8 Average daily driving distance in DK [32]

3.4.3 Charging power levels

The duration of the EV charging is determined by the charger power level. There are 3 types of charging levels, depending on the power, as well as, where or how the EV is going to be charged. According to [33]the EV owners prefer the second charging level as it takes less charging time of the vehicle. Furthermore, the charging level 2 is chosen for this study with 11 kW power capability of charging, according to [33]. This high level of power can be achieved because most of the Danish houses have 3-phase electrical installation.

Table 3-3 Charging Power Level[34]

Level	Charger location	Typical use	Energy supply interface	Power level
Level 1 (Opportunity, 120V/230V)	On-board 1-phase	Home or office	Convenience outlet	Up to 2 kW
Level 2 (Primary, 240V/400V)	On-board 1 or 3 phases	Dedicated outlets	Dedicated outlet	4-20 kW
Level 3 (Fast, 480V/600V or direct DC)	Off-board 3-phase	Commercial filling station	Dedicated EVSE	50-100 kW

3.4.4 Charging Profiles

Regarding the charging profiles, for this project two profiles have been chosen. One of them is called ‘Dumb Charging’, where the owner comes home and starts charging the EV immediately and the other one is called ‘Smart Charging’ or ‘Controlled Charging’, where with the help of the DSO the EVs charge during the night, lowering the stress on the system, as well as providing economical profit, due to charging at a cheaper price electricity hour.

3.4.5 Consumption needed for EVs

According to [32] the average consumption of a normal electric vehicle ranges between 0.12 kWh/km and 0.22 kWh/km. For this thesis, the energy needed for one EV is considered 0.22 kWh/km. From this and from the average distance found earlier in subchapter 3.4.2, the average energy needed for each EV in one day can be calculated as:

$$E = 0.22 \text{ kWh / km} * 48 \text{ km} \quad (27)$$

From the above equation it can be concluded that the average energy needed for each EV is approximately 11 kWh.

3.5 Summary

This chapter focus is the description of the generation and load part used in this master thesis. Different methods are used in modelling these parts in order to have a high accuracy. The input data, such as wind speed or solar irradiance, give the power curves of the generation, as well as from the measured thermal output power of the heat pump and the electricity consumed, the efficiency can be calculated. This project is focusing mostly on the system behavior, meaning that most of the EV parameters presented above were taken as average values.

4 Maximum Allowable Renewable Integration with and without Heat Pump Integration

In this section, the maximum allowable renewable integration must be found. In order to do this, the voltage and transformer/line loadings must be kept between the established boundaries.

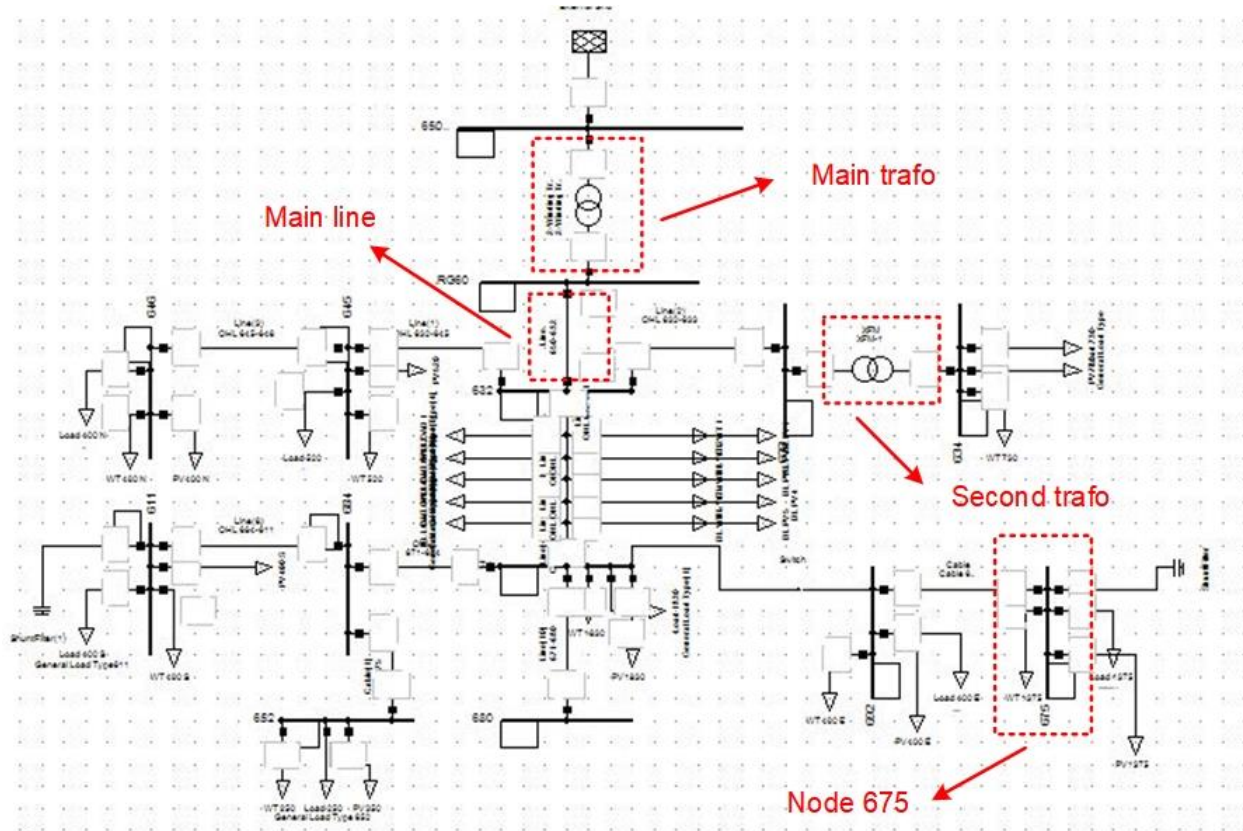


Figure 4-1 The Critical Components of the system

The system limits of the main components shown in the figure above are presented below:

- Voltage limit – this voltage limit consists of the limit set between 0.95 and 1.05 p.u. For this limit, the Node 675 will be analyzed. This node is chosen in particular as it is seen later in Figure 4-3, that this is the weakest node. This is required in order to see the fluctuations of the voltage (measured in p.u.).
- Main Line Loading – to not overload the lines and cause heating problems, this limit should not exceed 100%.
- Main Transformer Loading- (HV side 115-4.16 kV LV side) presented in Figure 4-1, the main transformer is shown. This is required to see the loading factor of the transformer in the different scenarios investigated (measured in %). The transformers loading limit

should be kept under 100%, in order to not cause problems such as gassing of the transformer.

- Second Transformer Loading- (HV side 4.16 – 0.48 kV LV side) Same as above, the loading factor will be studied for this case.

To find this value, the generation is increased for one day until one of the limits specified in chapter 1 is violated, or decreased if the limits are already violated, until the upper critical limit is reached. This procedure is conducted for two different seasons, January and July. These seasons are chosen due to their difference in load consumption throughout a day.

4.1 Household consumption

Initially, the base household consumption for January and July is present. The consumption in normal houses depends directly on the number of persons living in the house. Therefore, the consumption data is taken from with three different profiles, low, medium and high. Further, there are presented the number of persons for each category, as well as the percentage of the final consumption they represent, according to [35]

- Low Consumption = One Person (30% of final consumption)
- Medium Consumption = Male + Female + one children (51% of final consumption)
- High Consumption = Male + Female + three children (19% of final consumption)

Furthermore, in Figure 4-2 the curves are presented, with the averaged curve being the one which will be used further in this project for January and July, respectively.

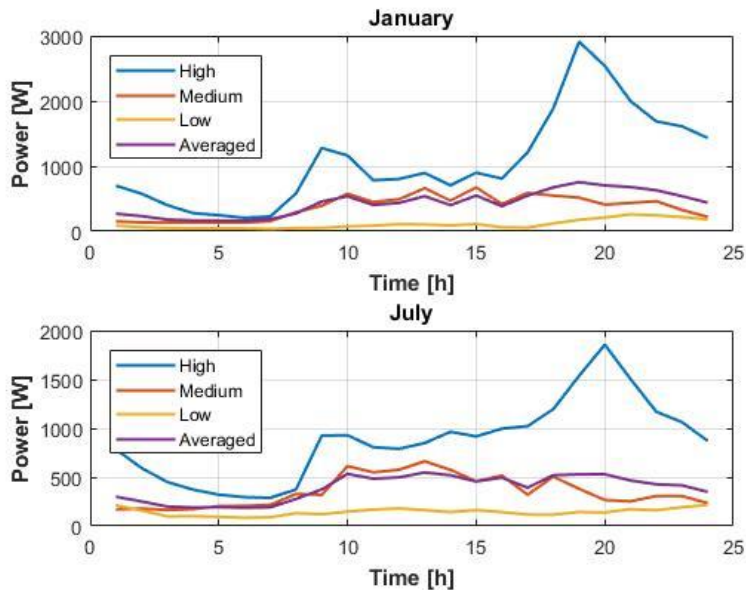


Figure 4-2 Household Electricity Consumption January/July 2013

Moreover, the number of houses at each node is established by keeping the load power close for each node to the validation power. Another criterion was to keep the transformer loading at around 70% with just the consumption.

Table 4-1 Node vs Houses

Node Number	Nr. Of Houses
646	400
645	520
634	730
671	1830
611	400
692	400
675	1375
652	250

In Table 4-1 it is shown the number of households for each node. In total, there are 6405 houses, totaling a consumption energy of 59 MWh for July case and 66 MWh for January case, for one day.

4.2 Maximum Renewable Integration

4.2.1 January Case

According to Chapter 1, currently, there are 2444 wind turbines with the rated power below 25 kW (residential scale), and 22 851 of PV panels with the rated power below 6 kW (residential scale) in Denmark. The ration between them is 1 wind turbine to each 9 PV panels. This ratio between WT and PV is taken for each case.

With this ratio calculated, the number of wind turbines and photovoltaic panels is increased, and 4 different cases are shown. It is observed that in the fourth case, the maximum renewable integration is found for January.

- a) Case 1:1 WT and 9 PVs every 10 houses; (640 wind turbines and 5764 PV systems)
- b) Case 2: 1 WT and 9 PVs every 40 houses; (160 wind turbines and 1441 PV systems)
- c) Case 3: 1 WT and 9 PVs every 90 houses; (71 wind turbines and 640 PV systems)

d) Case 4: 1 WT and 9 PVs every 160 houses; (40 wind turbines and 360 PV systems)

In Figure 4-3 it can be seen that in first case (case 1), the voltage for all busbars is violated. Further, in case 2 and 3 the voltage is still not respecting the limits. Although for case e-3 (third case) an overvoltage is present just at node 675, meaning that this node is the weakest node of the system. By identifying the weakest node, all voltage checks will be referred to node 675 in order to establish the stability of the system.

The fourth case, with 1 WT at every 160 houses and 9 PV at every 160 houses, the limits are still situated in the accepted range.

In Figure 4-4, the voltages for each hour of the day and for each case are presented, the base case (no generation) being taken as a reference. It can be observed that most of the voltage violations occur during the night, from 01:00 to 06:00 A.M., while in the rest of the day the voltage is situated between accepted limits for all cases.

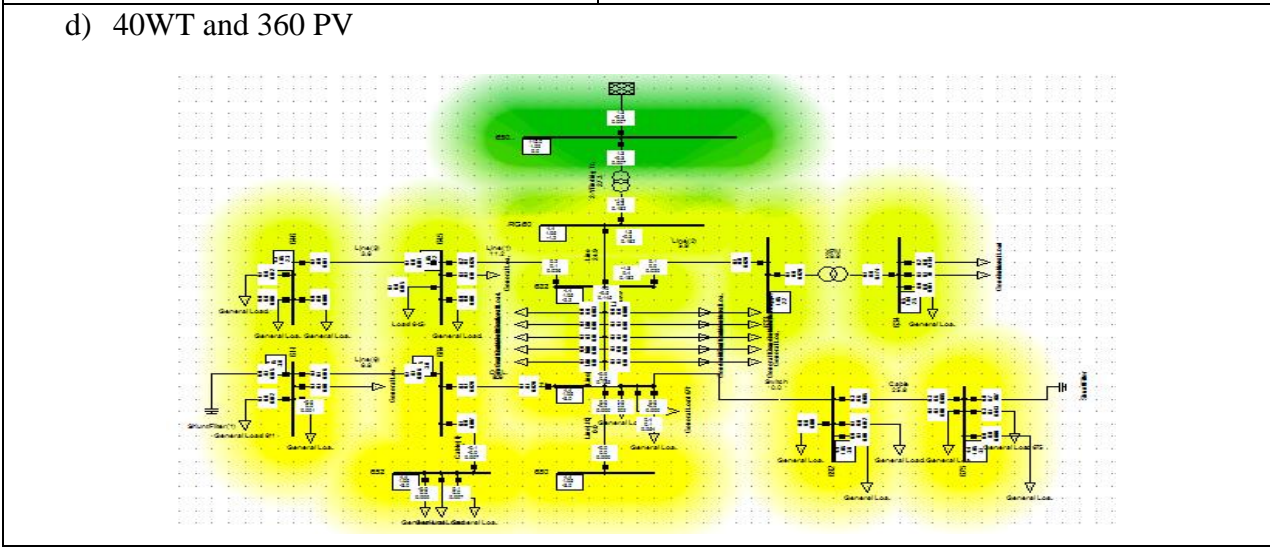
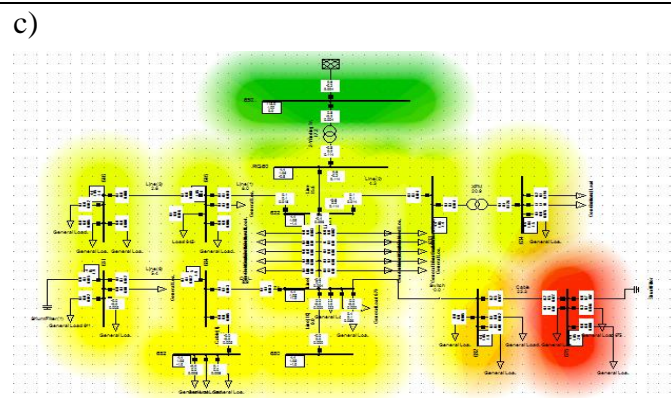
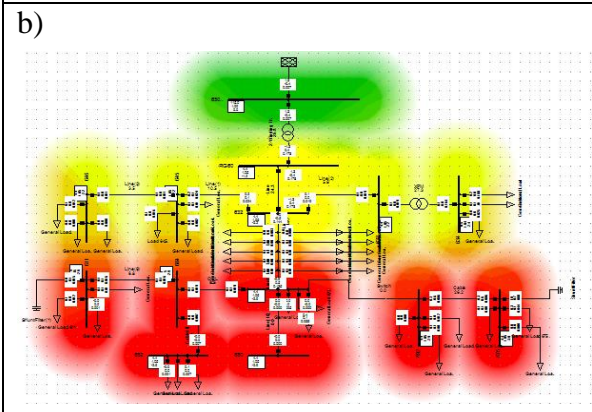
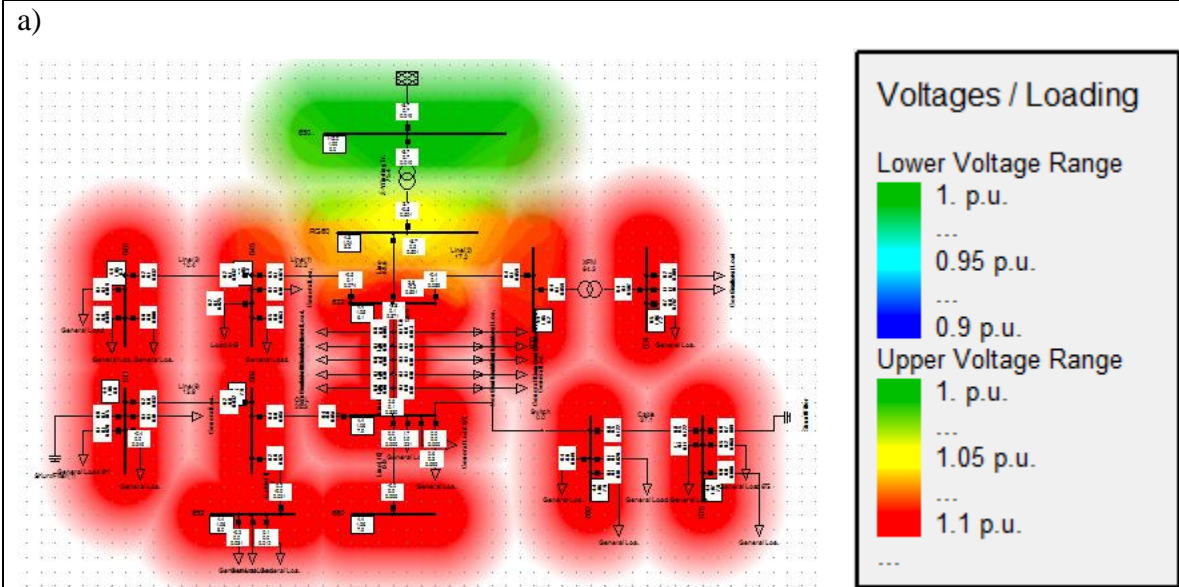


Figure 4-3 Max Renewable Cases 1-4 January

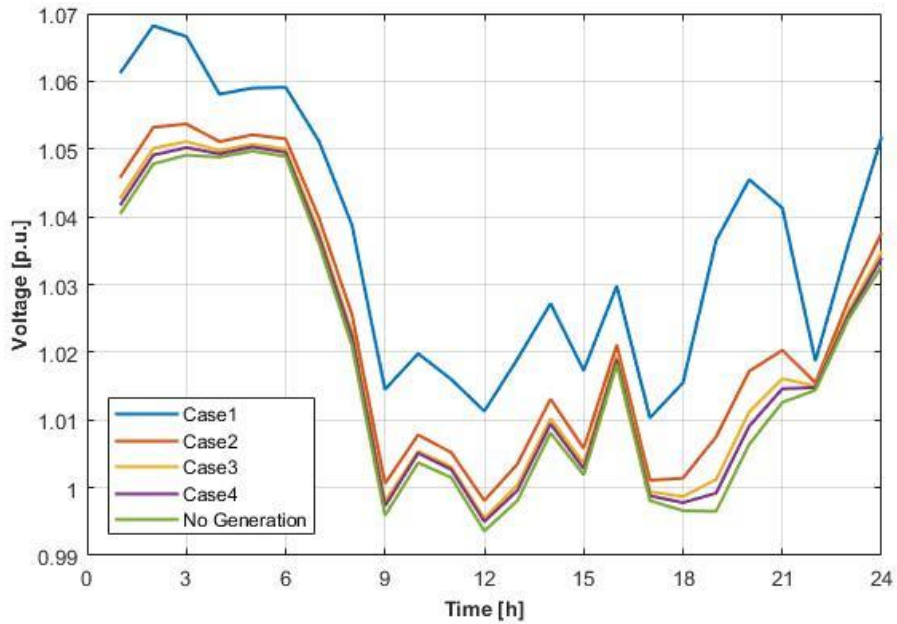


Figure 4-4 Node 675 Voltage Levels January

It can be seen in Figure 4-4, that due to the transformer tap ratio, the voltage is close to the 1.05 limit, in the night period, even for the base case (no generation). This will affect severely the generation, mainly because the voltage limit will be violated fast.

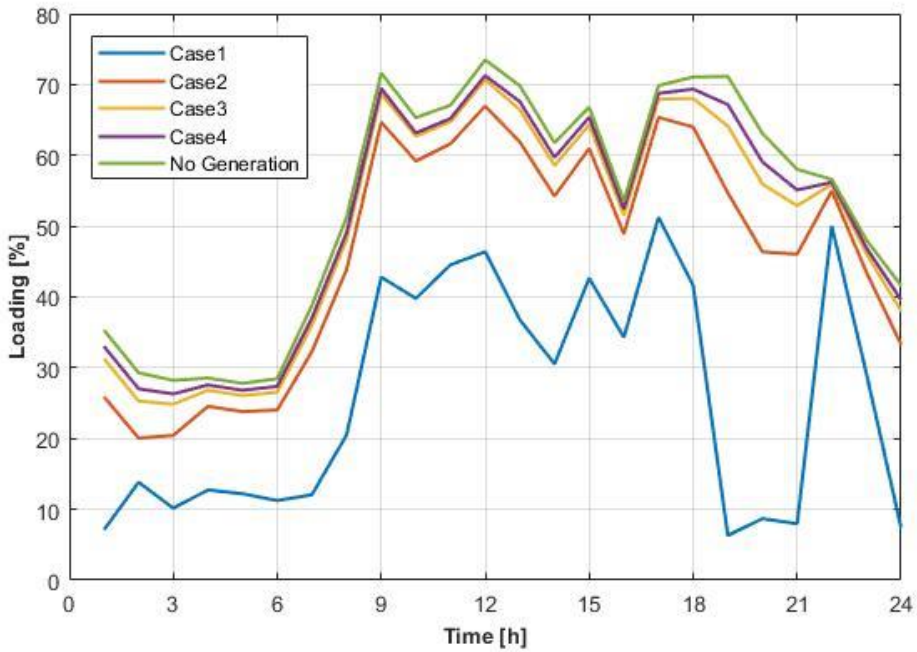


Figure 4-5 Transformer Loading January

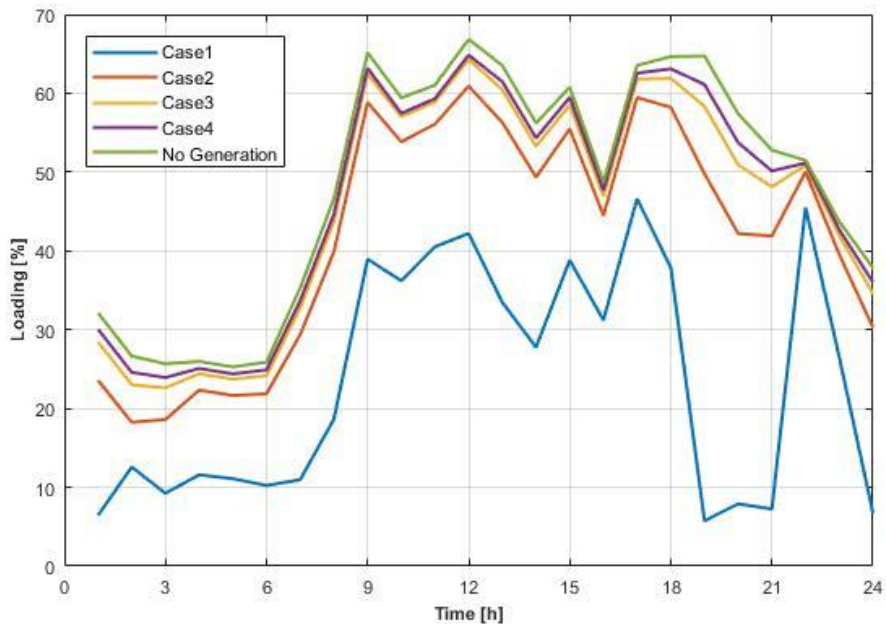


Figure 4-6 Line Loading January Case

In Figure 4-5, the main transformer of the system is presented. Its role is to connect the system to the outside grid. In this figure it can be observed that all the other cases have a lower transformer loading compared to the base case (no generation). Case 1 presents the lowest transformer loading, 10% during the night and 40% during the day. This is because of the large amount of renewable generation which supplies the local consumption and relieves stress from the transformer, due to less power going through it.

In Figure 4-6 the line loading is presented. The loading profile is similar to the main transformer profile, due to the fact that this line is connected directly with the transformer.

In Figure 4-7, the maximum renewable power generation from 40 wind turbines and 360 PV panels is presented (case 4). Although the number of WT is 9 times less, it can be observed that the maximum is recorded in the evening, with 220 kW from 08:00 to 09:00 P.M. which is provided just by the wind turbines

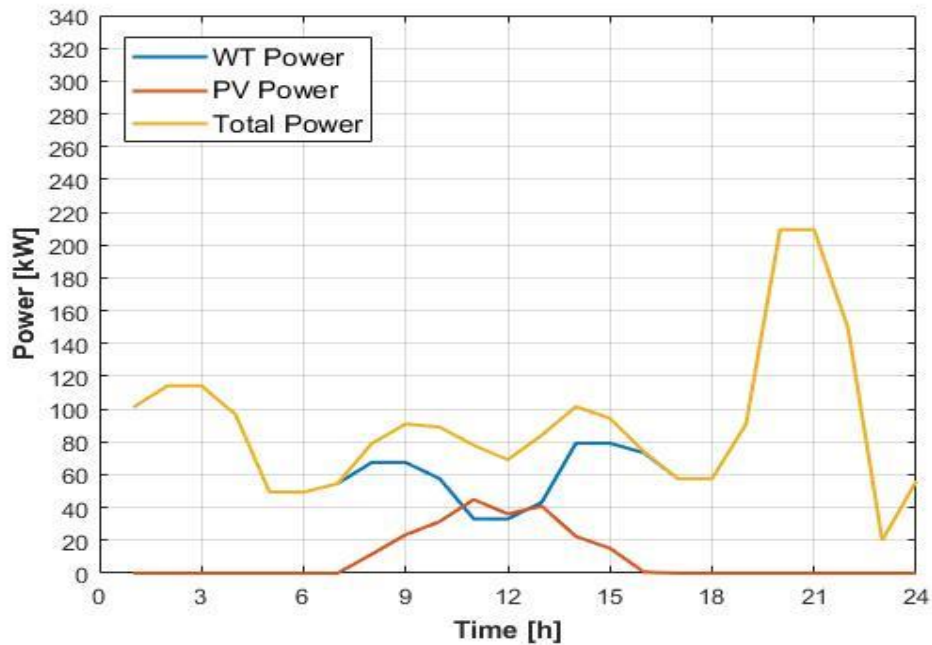


Figure 4-7 Max Renewable Generation (WT+PV) January

4.2.2 July Case

For this case, the same ratio of 1 WT:9 PV is considered, as well as the 4 cases where the generation is changed from case to case.

- a) Case 1: 1 WT and 9 PVs at every 10 houses; (640 wind turbines and 5764 PV systems)
- b) Case 2: 1 WT and 9 PVs at every 15 houses; (427 wind turbines and 3843 PV systems)
- c) Case3: 1 WT and 9 PVs at every 80 houses; (80 wind turbines and 720 PV systems)
- d) Case 4: 1 WT and 9 PVs at every 105 houses; (61 wind turbines and 549 PV systems)

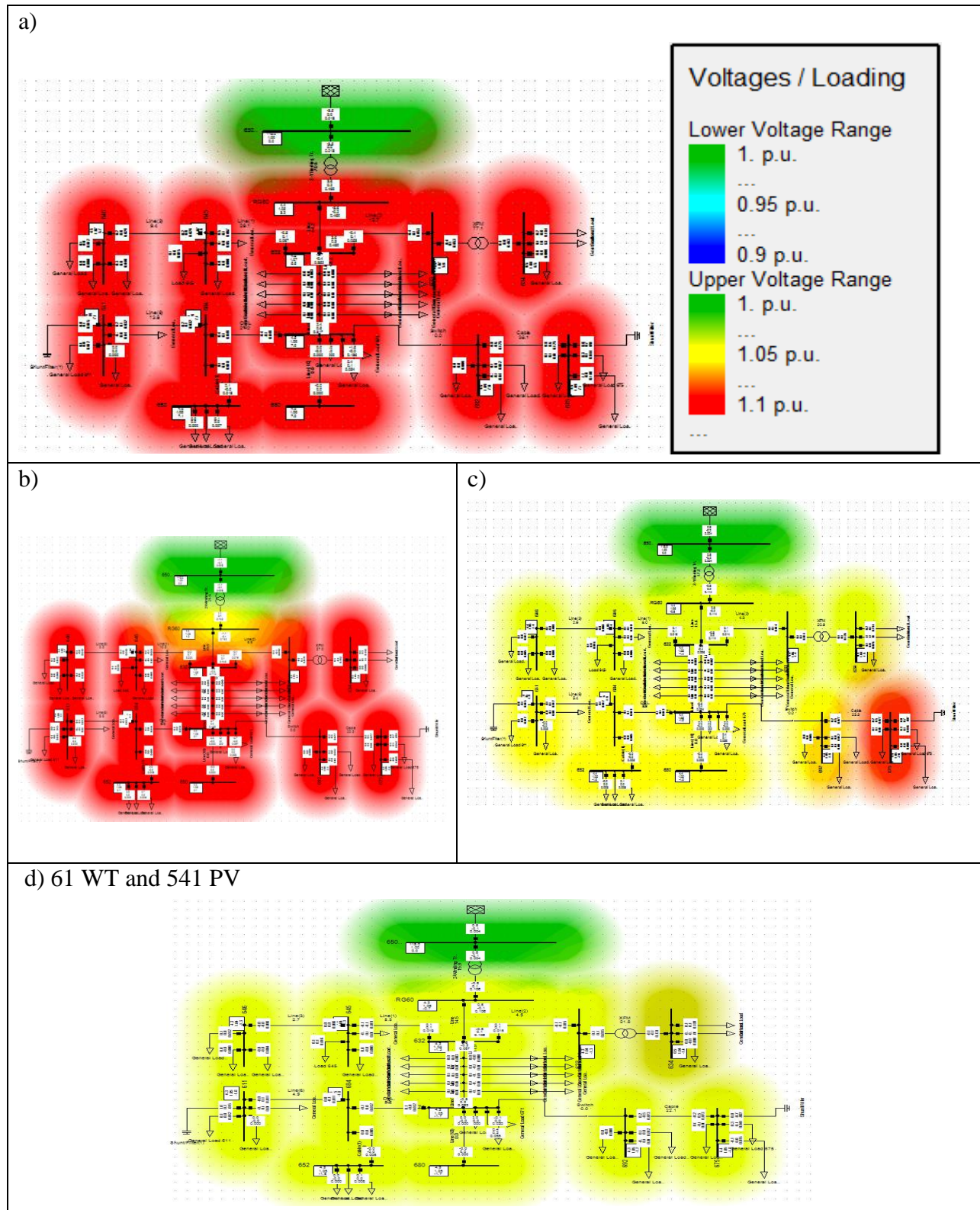


Figure 4-8 Maximum Renewable integration July

The 4 cases and their behavior are shown in Figure 4-8. The same procedure as in January case is followed. The voltage limits being violated for all the busbars in the first case, the generation is

decreased case by case until the optimal one is found. It can still be seen that in case 3 (third case) bus bar 675 is still the only one with its limit violated.

In Figure 4-9 the transformer loading is presented, with the same behavior as presented in the January case, lower loading for a bigger generation. This is due to the distributed generation (WT and PV) feeding power to the consumers locally, lowering this way the power needed from the grid, releasing stress of the transformer.

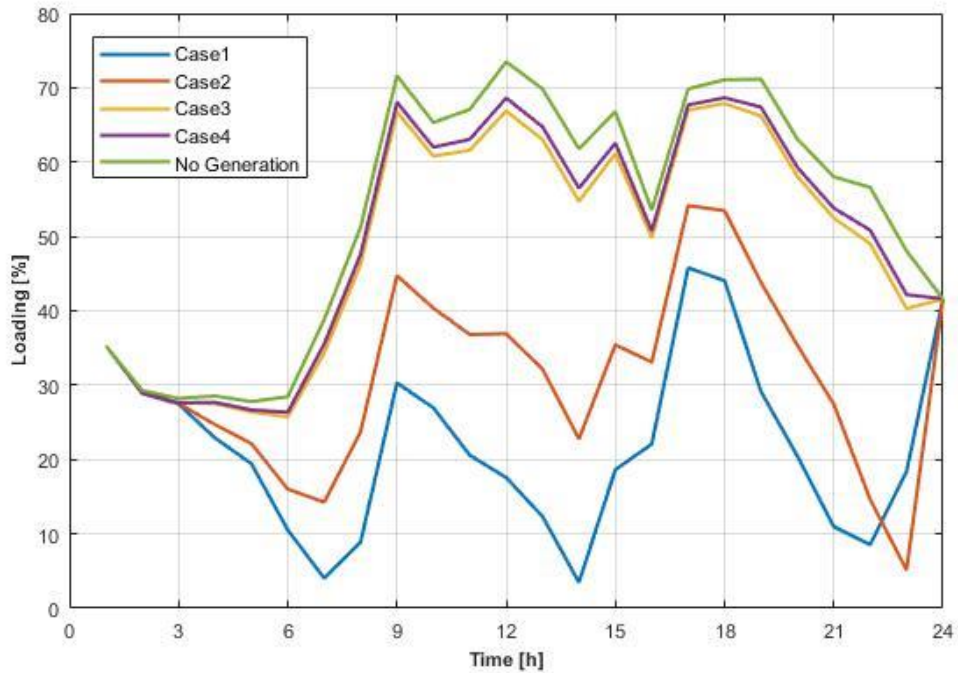


Figure 4-9 Transformer Loading in July

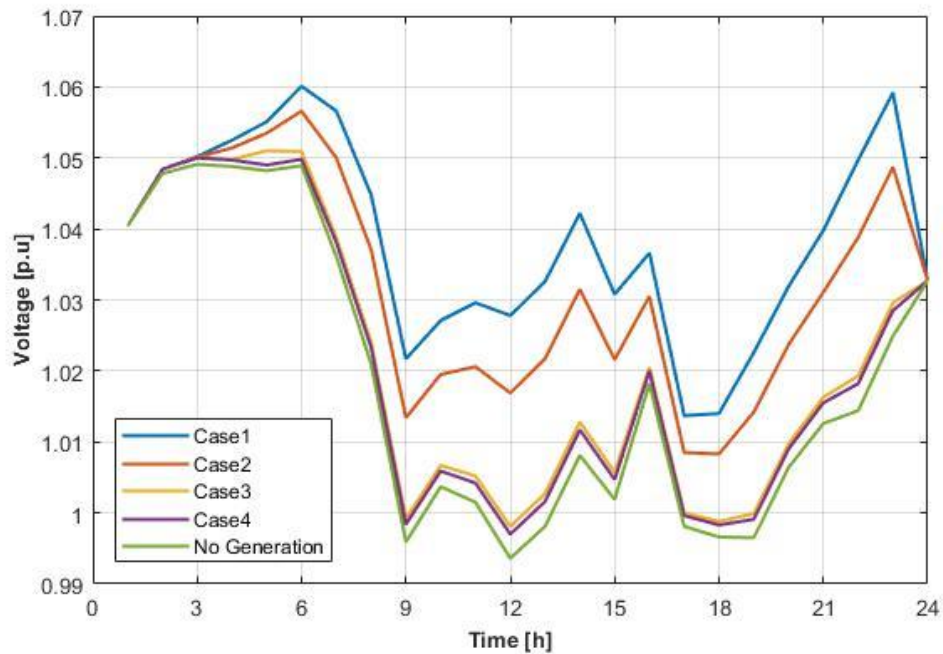


Figure 4-10 Node 675 Voltage in July

In Figure 4-10 the voltage profile for all the cases is represented. Compared to the January case, the July case is similar regarding the period where the voltage violations occur, this being from 01:00 to 06:00 A.M. For the 17-18 it can be seen that comparing to the other hours, this hours is the heaviest loaded, having the smallest amount of p.u. voltage, 0.995.

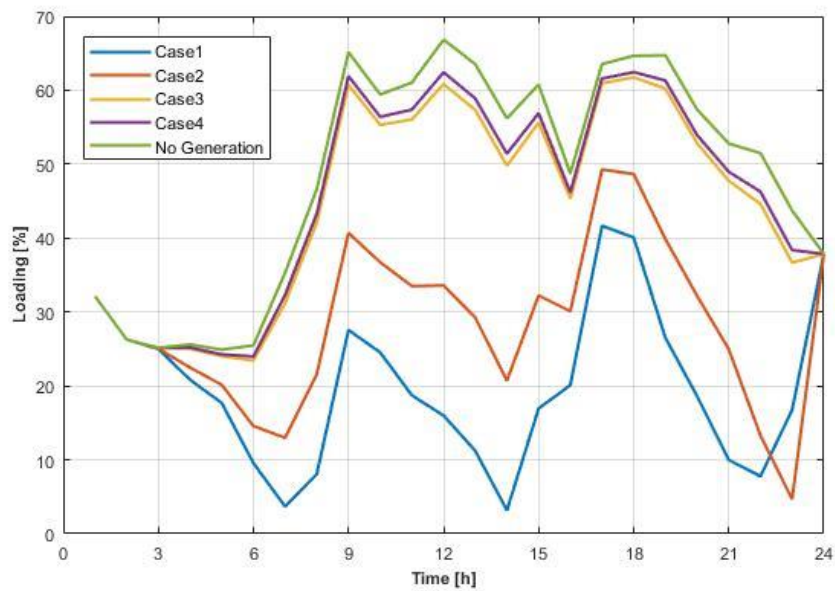


Figure 4-11 Lines Loading July

In Figure 4-11 the loading of the main line connecting the main transformer with the system is shown. This line was chosen because it has the most loading stress compared to all the other lines in the system. It can be observed that it has the same behavior as the transformer loading, having its loading reduced as the generation increases.

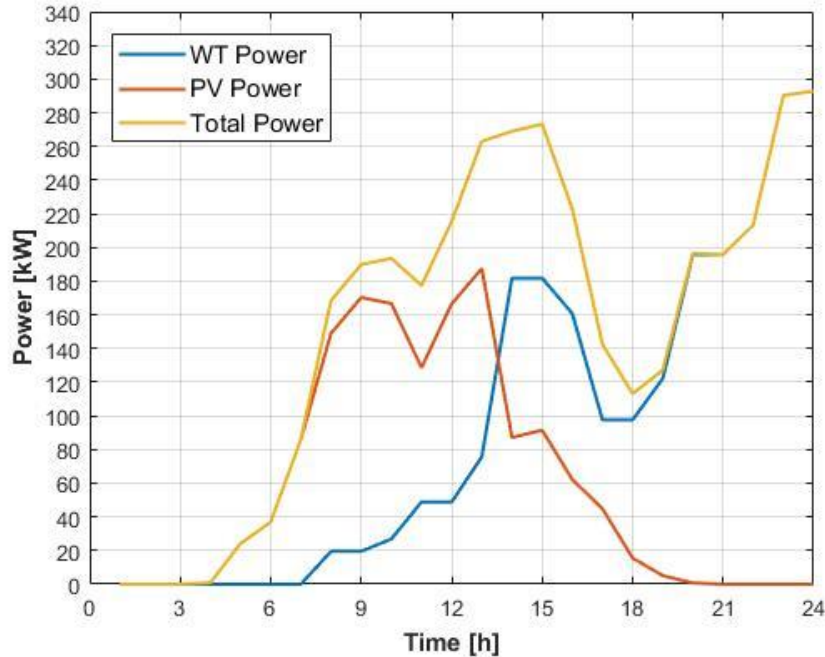


Figure 4-12 Renewable Maximum Generation July

The maximum renewable generation for July is depicted in Figure 4-12. This generation is produced by 61 wind turbines and 549 PV panels, which is higher than January case (40 WT and 360 PVs). Although, the generation of the wind turbines for a day in July is smaller than a day in January, with 21 more wind turbines in July, compared to the previous case, the power generation increases with 80 kW around 12:00 A.M, reaching 300 kW. To keep a valid comparison between January and July, the number of WT and PV systems in July is lowered to the numbers of WT and PVs in January case.

4.3 Integration of Heat Pumps in the system

As stated in previous chapters, heat pumps are good to store the extra energy as heat, being extremely useful in periods of high wind penetration. According to the Danish Energy

Agency[36], around 12% of the total houses have heat pumps in Denmark. Regarding this project, the number of heat pumps is taken with the same percentage, totaling a number of 768 heat pumps.

As seen in 4.2, the main limit of the renewable integration is the voltage upper limit. Integrating heat pumps, which are acting like loads, the voltage decreases, giving the opportunity for more renewable generation to be added.

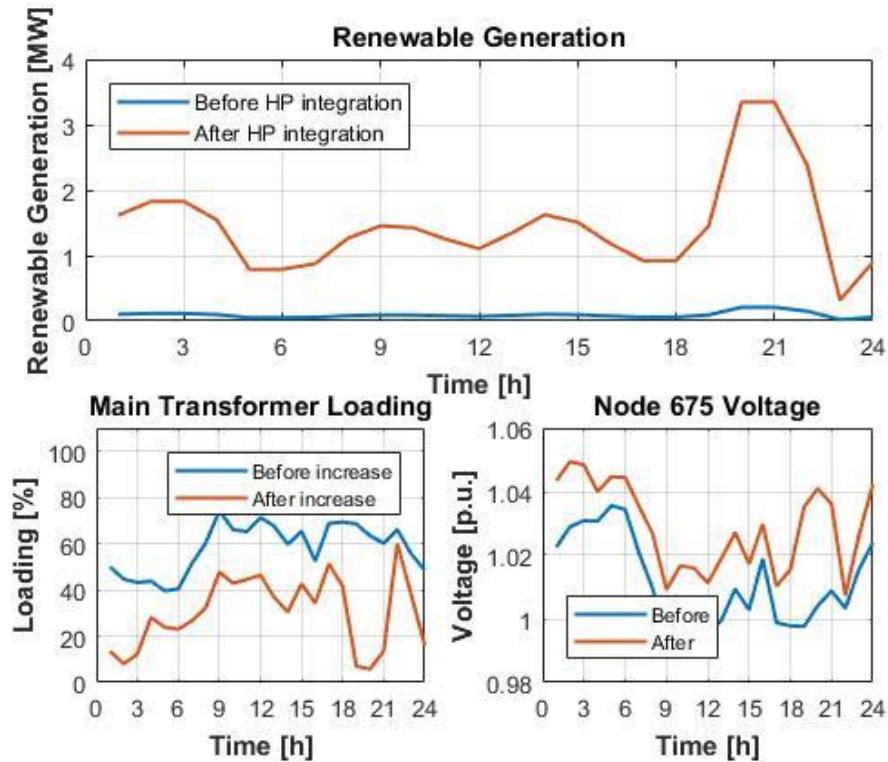


Figure 4-13 New Maximum Renewable Generation January

The total energy for a day in January required by the heat pumps is 8.2 MWh. This added load, allows for the January case an increase from 1 WT and 9 PV at each 160 houses, to 1 WT and 9PV at every 10 houses. The new numbers being 640 wind turbines and 5764 PV panels.

In Figure 4-13, the new renewable generation is presented in the upper plot, where it can be clearly seen the astonishing difference between maximum renewable generation with and without heat pumps. Secondly, the transformer loading as well as the voltage profile are presented before and after the new maximum renewable generation is integrated. With the help of the heat pumps, the voltage drops from being approximately constant at 1.05 p.u. during the night, as shown in Figure 4-4 in chapter 4.2, to approximately 1.03, allowing this way for more renewable integration.

It has been concluded in 4.2 that January case can integrate fewer number of WTs and PVs than July. For a fair comparison between January and July, the same number of wind turbines and PV panels is required for both cases (40 WTs and 360 PVs). Before the heat pump integration, the number of WTs and PVs in July is adjusted to the numbers considered in January. Because adding the heat pump in January permits considerably more renewable energy integration (640 WTs and 5760 PVs), a new number of WTs is set, according to the maximum renewable energy integration in July. The final number of WTs and PVs is 61 and 549, respectively. The power production in January before the heat pump integration and the new limited power production according to July is shown in the figure below.

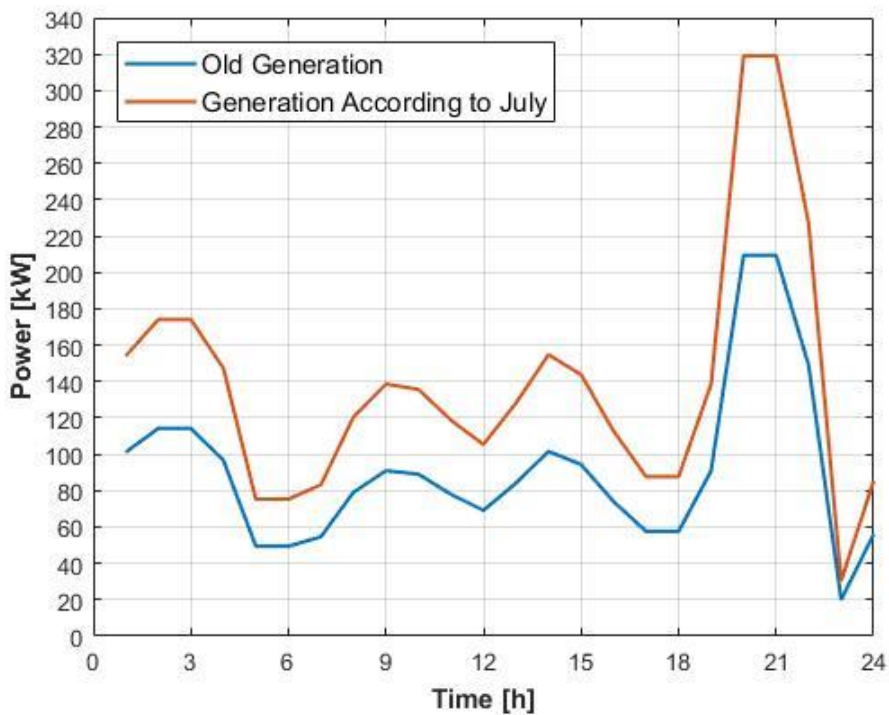


Figure 4-14 Old vs New Generation January

4.4 Summary

In this chapter, the number of households is determined by adjusting the power to match the one in the IEEE 13 bus network consumption power. Furthermore, the maximum renewable generation for January and July is found. This maximum is limited mainly by the voltage at node

675, available for both cases. It is shown that January can integrate fewer wind turbines and PV panels than July. This is due to a higher generation in the January case. To select the number of WTs and PVs between the two cases, the case which can integrate fewer systems is chosen as a reference (40 WTs and 360 PVs).

Moreover, the weakest busbar of the system is found, represented by node 675, therefore all voltage analysis is performed on this node. By finding it, lower simulation time is required for future analysis of the system.

Regarding the heat pump integration, it can be seen that the renewable generation increases to 1WT and 9 PV at each 10 houses reaching 66 MW compared to 1WT and 9 PV at every 160 houses, reaching 4 MW. The final number of WTs and PVs is found by taking the maximum renewable integration in July case as reference (61 WTs and 549 PVs).

5 Control Methods to Increase Maximum Allowable Renewable Integration

To increase the maximum allowable renewable integration control methods are conducted and analyzed. In this master thesis, active and reactive power control are implemented to the wind turbines power.

5.1 Active Power Control

As stated in the previous chapters, the interest in wind power is on a continuing rise. Having the distributed generation on residential areas rising, makes the system more stressed. In this project it was seen that the system allows 61 wind turbines, which is one turbine at each 105 houses for both January and July. To be able to integrate more, control methods must be applied to the system. First control method to be studied is the active power control. This control method is based on connecting more wind turbines to the system, by limiting the active power for the hours where one of the limits is violated. In the flowchart, the increased WT number is represented by x , measured in percentages with regards to the based WTs number (61 WTs). The steps taken for this control are presented in Figure 5-1:

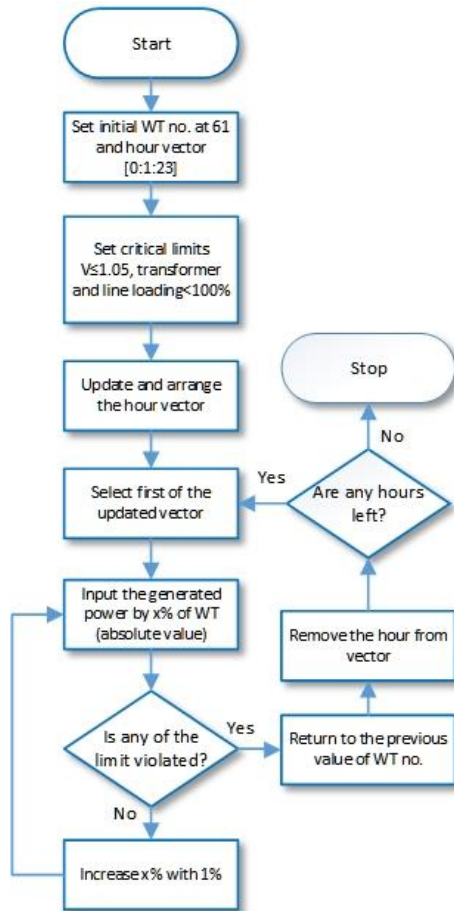


Figure 5-1 Active Power Control Flowchart

Firstly, the base number of wind turbines (61 WTs) and the hour vector (hour 00 to 23) are generated. Secondly, the voltage and loading limits are set. Thirdly the first hour of the updated vector, is selected. At this particular hour, an input of “x %” of WT is given. For the start of the simulation, x % is equal to the 61 WT. Following this step, the limits are checked. On one hand, if the limits are violated, the x % returns to the previous value. After, the hour at which the simulation took place is removed from the vector. Next, a new check is made, regarding the hours in the vector. The simulation is stopped when the vector with hours is empty. If the vector is not empty, the hour vector is updated, and the simulation starts again, with on this hour. On the other hand, if the limit is not violated, the number of WT “x %” is increased with 1 % (always the number of WT will be an absolute number) and it is added to the system, where the limits are further checked.

The maximum number of wind turbines that can be integrated in the system is simulated, for both January and July.

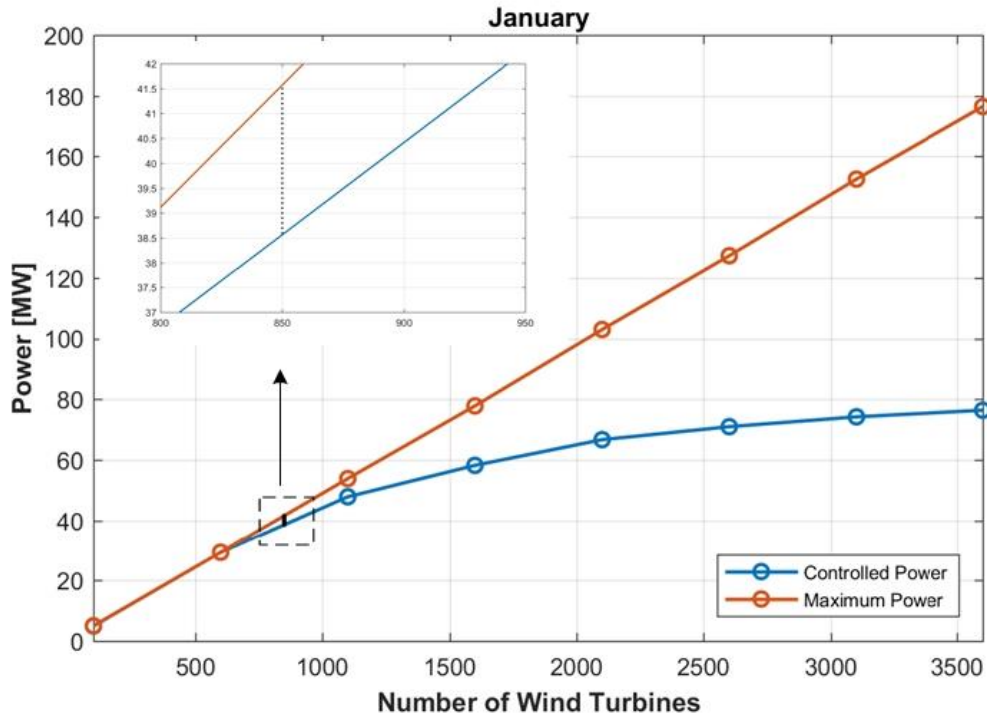


Figure 5-2 Max WT January

The method to find the number of wind turbines is to add wind turbines and limit the power where the conditions are violated. This is done until the curtailment ratio of Wind Power reaches 7 % according to [37] as seen in Figure 5-2 for the January case. It was discovered that the number of wind turbines at which the curtailment ratio is 7% is 850 Wind Turbines, producing with active power control 38,523 MW, meaning 1 WT each 7 houses. The black dotted line represents the curtailment between the controlled power curve and the un-controlled power curve.

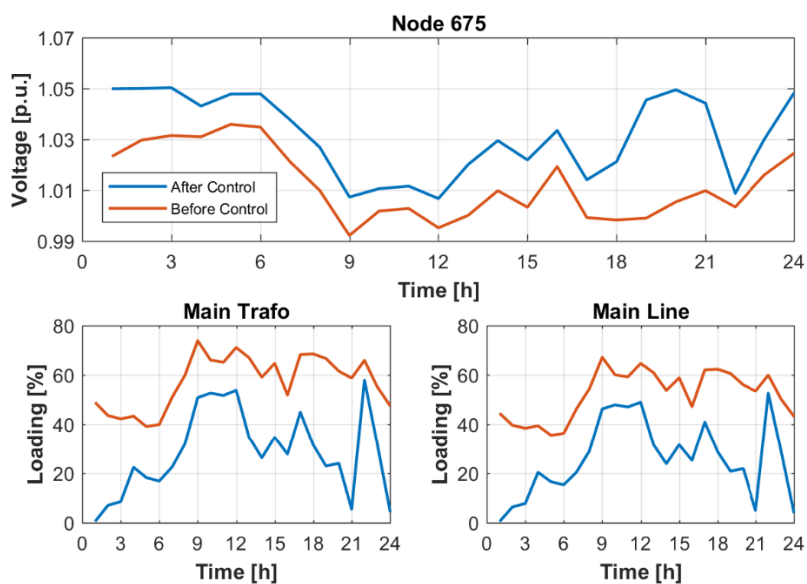


Figure 5-3 Voltage, Transformer and Line profiles for 850 WT (January)

In the above Figure 5-3, the profiles of the voltage, transformer and line loading are presented for January case. In the first plot it is represented the voltage at node 675 after the control scheme was conducted. It can be seen that for some hours of the day (00:00-03:00 a.m. and 08:00-09:00 p.m.), the voltage is equal to 1.05, which represents the upper limit. For the transformer and line loadings, after the control was performed (the blue line), the loading has decreased, mainly because of the amount of renewable power generation is higher than the consumed power, therefore the supplying is done locally, meaning that the power is not required to go through the main transformer. For the case with 3600 WT (January and July), the voltage profiles are presented in Appendix.

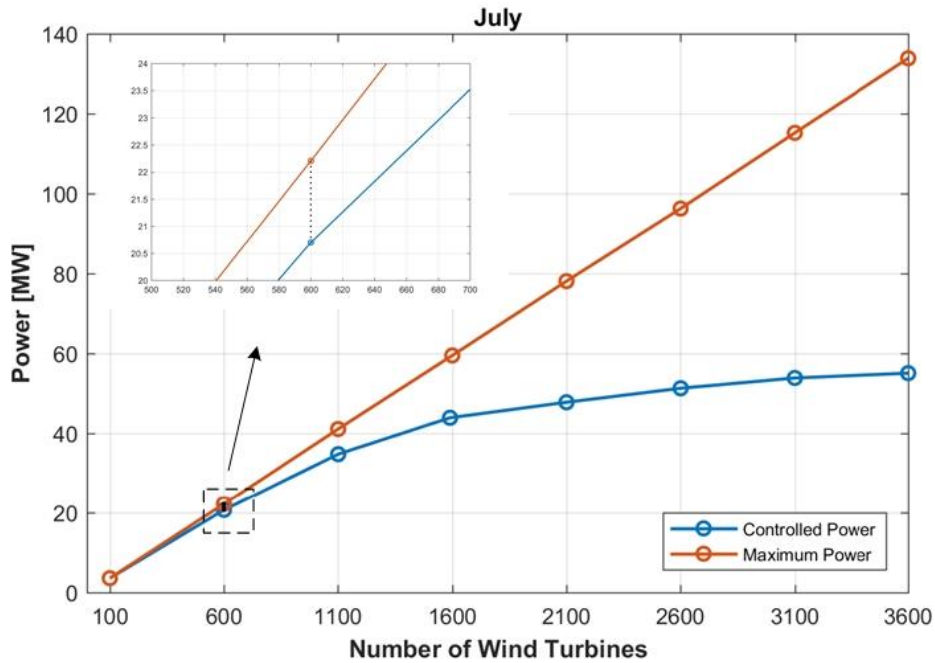


Figure 5-4 Max WT July (600 WTs)

In Figure 5-4 the active power control for July case is presented. The control was done as in the January case, with the stop point being at 7% of the curtailment ratio. It has been found that for 7% of the curtailment means 600 Wind Turbines, and 20.7 MW, meaning 1 WT each 10 houses. The curtailment is marked by the black dotted line.

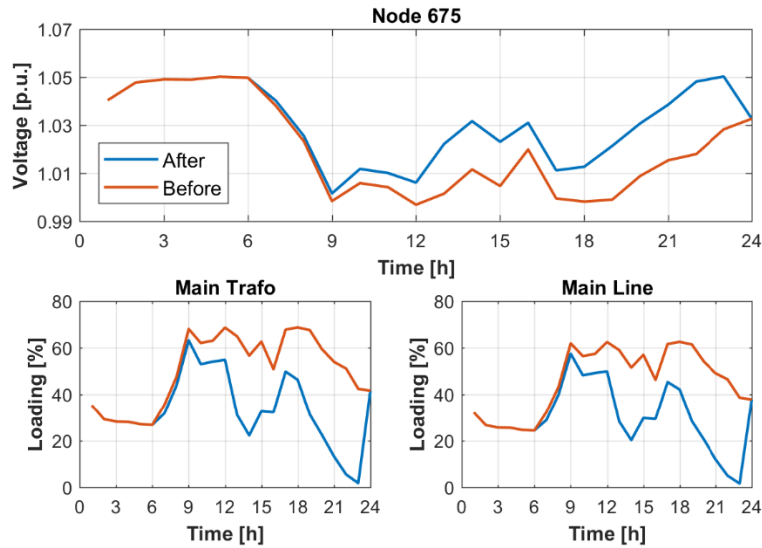


Figure 5-5 Voltage, Transformer and Main Line profiles for 600 WTs (July)

In Figure 5-5 the plots for July case are presented. Regarding the voltage, it can be seen that throughout the night from 1 to 6 a.m. the voltage was already at the maximum limit, meaning that no active power control is made in that period. This is one of the reason, why for July case there is less power produced. The transformer and line loading present the same behavior as in January case, having lower loading after the control is applied.

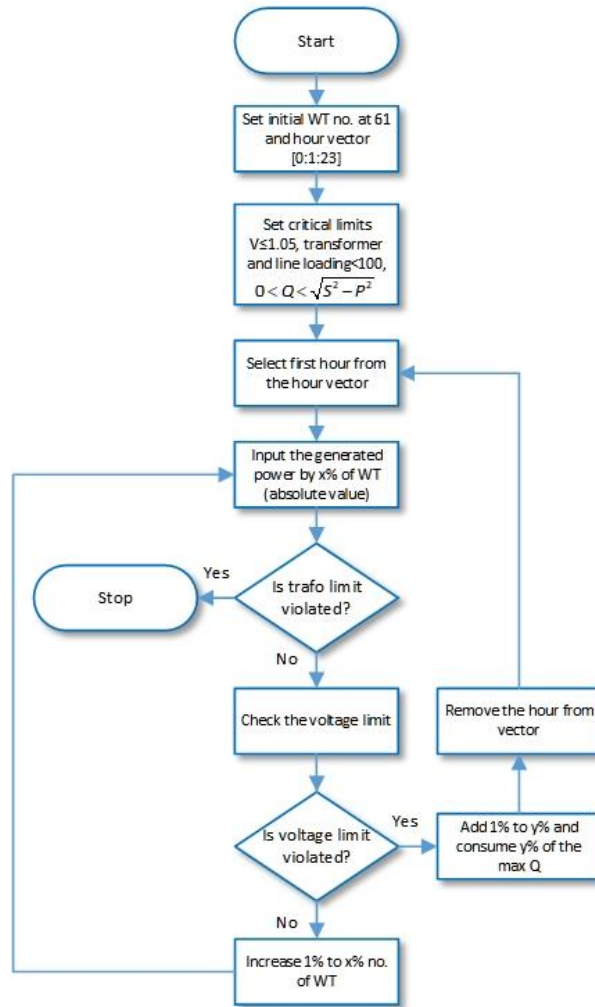
5.2 Reactive Power Control

Another method of controlling the power of WTs is Reactive Power Control, where in order to keep the voltage below the critical limits, when increasing renewable generation, reactive power is consumed by the converters of the wind turbine so that the voltage will decrease, and no limits is violated.

The constraints for this control are:

- Transformer Loading <100%
- Line Loading <100%
- $0.95 < V < 1.05$
- $0 < Q_{(i) \text{ consumed}} < \sqrt{S^2 - P_i^2}$

Where $S = 10$ kVA, and P is the amount of active power produced at hour(i) in kW, as well as Q being the amount of reactive power consumed at hour (i) measured in kVAR.



Firstly, the base number of wind turbines (61 WT) and the hour vector (hour 00 to 23) are generated. Secondly, the limits are set, with $0 < Q < \sqrt{S^2 - P_i^2}$ being the maximum reactive power that the wind turbine can generate, with S being 10 kVA, and P being the power produced at hour i by the turbine. Thirdly the power from “x% “of wind turbines is given as an input. Following this step, the transformer limit is checked, which is followed by a voltage check. The simulation is stopped when the transformer limit is met, due to the fact that the transformer loading can’t be lowered. On the other hand, if the voltage limit is violated, 1% of the maximum reactive power possible to consume from the Wind Turbines is added to the variable $y\%$. For the start of the process $y\%$ is considered 0%,

meaning the simulation starts with no reactive power consumed. Next, the hour where the reactive power was consumed, is removed from the vector containing the hours, and the next hour starts. If there is no limit violated, 1% more to the x% of Wind Turbine number, is added. (this value will be an absolute value)

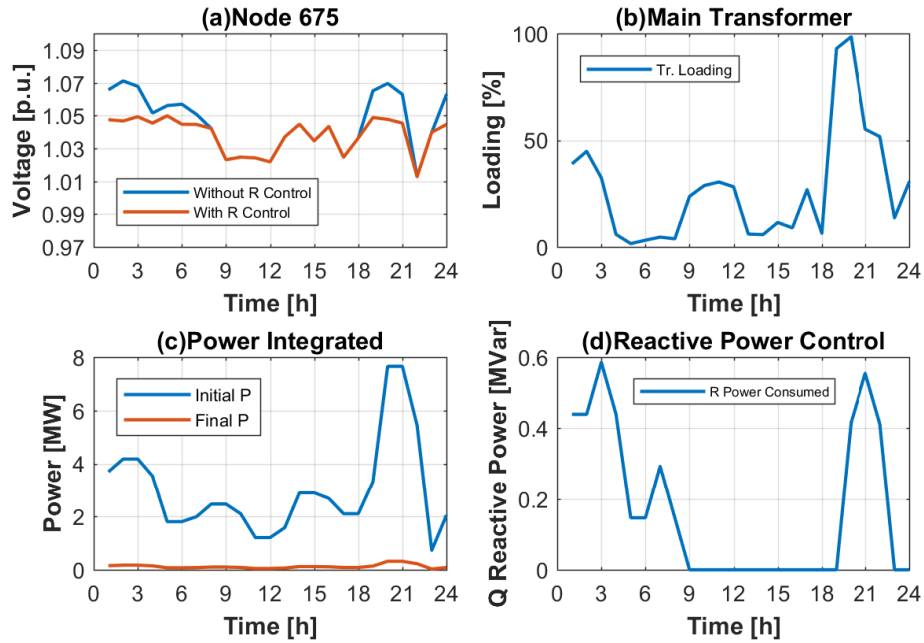


Figure 5-6 Reactive Power Control profiles (January)

In the Figure 5-6 the voltage is presented in the first subplot, (a). Without reactive power control, the voltage would violate the limits for the most part of the day (from 00:00-07:00 a.m), while with control, the voltage is kept between the bounds. In the second subplot (b), the transformer loading is presented, in which it shows that between 8:00-9:00 p.m. the transformer loading reaches 100%. This loading, limits the amount of integrated renewable generation possible to integrate in the system at 1464 wind turbines, with the total power at 71.79 MW. If the renewable generation would still be increased the transformer loading will increase over 100%, which if the loading is kept for a long period over 100% will damage the transformer. Third (c), the difference between the initial power provided by the base case (61 WT) and the new power, achieved with reactive power control is presented. Lastly, the amount of consumed reactive power is shown in (d).

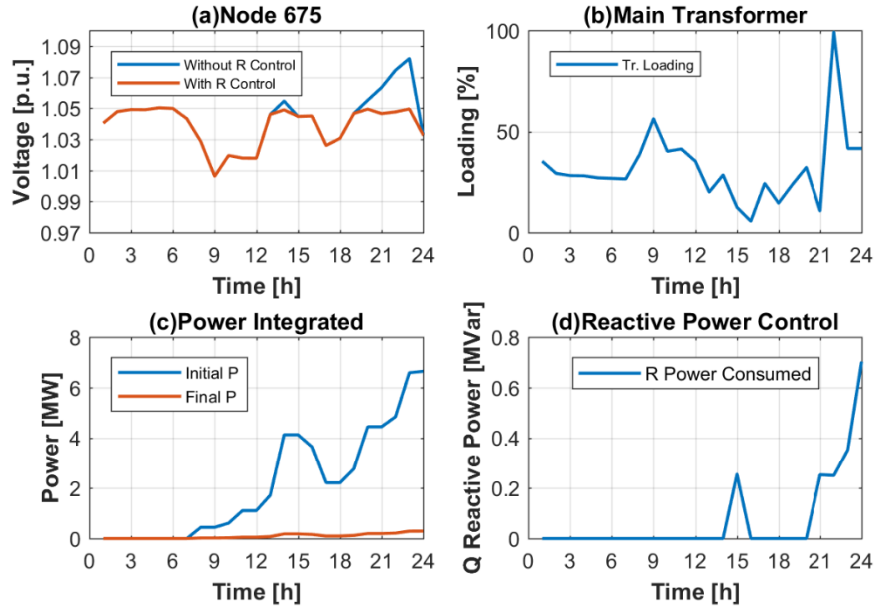


Figure 5-7 Reactive Power Control (July)

Regarding the reactive power control performed for the July case, it is found that the system can integrate 1384 WTs, (1 WT each 4 houses), totaling 51.48 MW. For the voltage profile shown in subplot (a), it is seen that for 12:00-2:00 p.m., and for 7:00-11:00 p.m. the voltage rises above the limit. Due to the reactive power control, the voltage remains below the 1.05 p.u. limit. For subplot (b) the main transformer loading is shown, reaching the critical limit at 11:00 p.m. stopping the increase in wind turbine number. For (c), the comparison between the power for July-base scenario (61 WT) and the power increase after the reactive power control is shown. For (d) the reactive power consumption is presented, showing the hours where it is needed for the wind turbines to consume reactive power.

5.3 Summary

In this chapter the active and reactive power control has been studied. Regarding the active power control, the maximum renewable generation is found to be 850 Wind Turbines, providing 35.29 MW for the January case. For the July case, 600 Wind Turbines were chosen based on the curtailment ratio, providing 20.7 MW. The difference between January and July can be explained in two ways. Firstly, the wind speed in January is bigger than July, meaning that more power will be produced. Secondly, in July case, the voltage is already near the voltage limit 1.05, while in January case, the voltage is at approximately 1.03 during the night, due to the HP integration, which lowers the voltage. The number of wind turbines that can be integrated with active power

control is of 600 WT (1 WT each 10 houses). This number is given by the July case, where the curtailment is reached faster than the January case.

Regarding the Reactive Power control, the voltage is controlled by consuming reactive power, keeping the voltage between the boundaries. The critical limit that limits the increase in renewable generation is the transformer loading. For the January case 1496 Wind Turbine can be implemented in the system, providing a total power of 54.4 MW. For July 51.48 MW can be achieved after implementing reactive power control, meaning 1WT each 4 houses. Seeing that in July, the number of WT is smaller, the reference case is taken as July, with 51, 48 M, meaning a WT at each 4 houses.

6 Technical-Economic Analysis

In this chapter, two different charging scenarios are tested. Dumb charging refers to charging EVs from 17 when most of the people arrive home. Firstly, 17 o'clock is picked for the start of the simulation because usually it is the highest loaded hour of the day regarding consumption. Secondly, the smart charging is performed based on the values of the lowest electricity price of the day, according to Elspot Market Prices. The integration of EVs is discussed both for January and July. The analysis of the system behavior after the EVs are integrated is discussed. Furthermore, the economic analysis is performed, in order to show the benefits of smart charging over dumb charging. For this purpose, the base renewable generation case (without heat pump or reactive/active control) is used, with 1 WT and 9 PV at every 105 houses, for both January and July.

6.1 January Case

6.1.1 Dumb Charging

Firstly, the dumb charging is performed, where the EVs are charged as soon as the owner arrives home. The equation used to determine the maximum allowable energy supported by the system at each busbar is presented next:

$$P_{\max,(i)} = \sum_{k=17}^n H_{(b)} * EV * Ch_p * x_{(i)} \quad (28)$$

Where $P_{\max,s}$ is the maximum supported power at each hour (i) to charge the EVs; H_b is the number of houses at each busbar (b represents the node number), where; EV is the total percentage of EVs (20% in this case); k is the start hour at which the EVs are considered to be home; Ch_p is the charging power required by the EV (11 kW taken for this project), and $x_{(i)}$ is the maximum allowed percentage of EVs to charge supported by the system for hour (i), shown in tables: Table 6-1 Dumb Charging % January, Table 6-2 Smart Charging % January.

In this case the starting hour is 17, which is usually the hour with highest power loading. The process of charging the EVs is explained in the figure below.

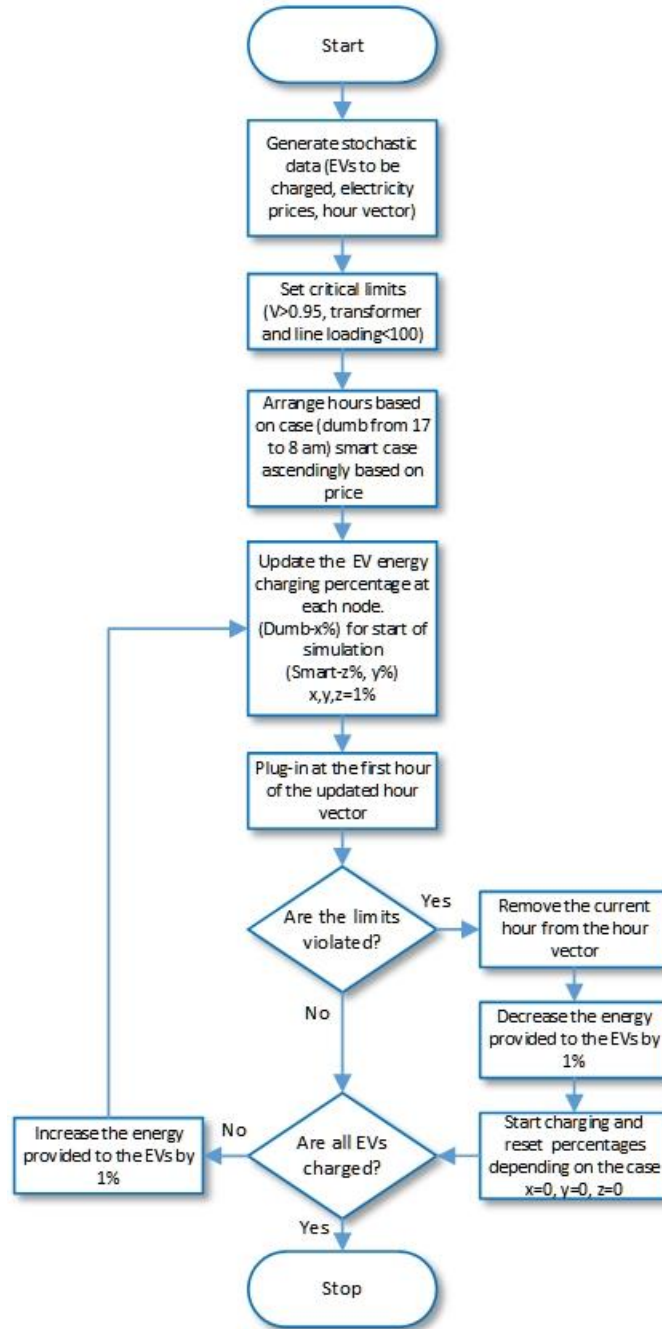


Figure 6-1 Simulation Method of EV Charging

In the above flowchart, the process of charging the electric vehicles for one day is explained for both dumb and smart charging.

Firstly, the data such as electricity prices based on Elspot Market as well as the vector with the hours of the day are input. Secondly, the three main constraints are set up: voltage, transformer loading and line loading. Thirdly, the hour vector is arranged based on the type of charging. Next

step is to start allocating percentage of the total EVs (x%, y%, z%) for each busbar, using equation (29),(30) and (31) depending on the case, , where (x% represents the total percentage number of EVs that are limited by the second transformer limit, for dumb charging case. In dumb charging, the only critical limit that is studied is the second transformer loading). For Smart Charging case, it is shown in Figure 6-3, that the loading of the second transformer is reached faster than the loading of the main transformer. z% represents the total number of EVs with regards to the main transformer, while y% represents the total number of Evs with regards to the second transformer. For the start of the simulation, 1% is chosen. Further, the limits are checked. If they are violated, the hour that the EVs were charging is removed from the vector, and the process is repeated for the following hour. On the other hand, if the limits are not violated, more energy is added to the initial 1%. After that, the limits are checked again. The iteration stops when there are no more EVs to be charged. In the table below, the maximum percentages of energy allowed by the system for each hour is presented. The critical limit that gives the maximum allowed energy to be supplied to the EVs is the second transformer loading, as shown in Figure 6-2 Dumb Charging January

Table 6-1 Dumb Charging % January

DUMB CHARGING		
i	Hour (i)	Percentage of Max P according to the Second Transformer $x_{(i)}$ (%)
1	17	7
2	18	7
3	19	8
4	20	10
5	21	11
6	22	8
7	23	12
8	24	15
9	1	14
10	2	8
	Total	100

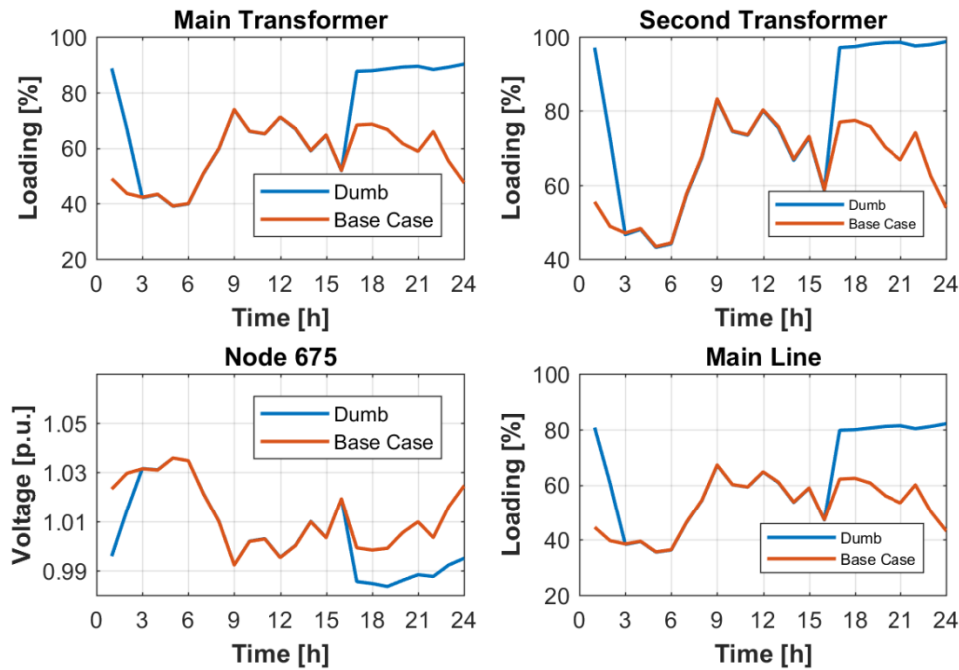


Figure 6-2 Dumb Charging January

In the figure above, the loadings and voltage of the critical components in the system are presented for the dumb charging in January case. To have a better understanding, of the effect of dumb charging, the base case profiles are also shown.

In the period of charging the EVs from 17 to 2 as shown in Table 6-1 Dumb Charging % January, the loadings of the transformers and lines have drastically increased. The first violation that occurs when trying to charge the EVs is the loading of the second transformer, rising at 100% while the main transformer for the same energy required, rises around 90%. In subplot 3 the voltage profile of busbar 675 is presented, showing that even in the period of the charging when the voltage drops, it still remains in the limits, reaching just 0,99 p.u. For this case, the loading of the main line is between boundaries, reaching just 80% in the charging period.

6.1.2 Smart Charging.

Analyzing the flowchart mentioned above, it is seen that the iteration with regards to adding 1% more to the number of EVs that can be charged, stops when one critical limit is violated. For dumb charging, it is seen that the second transformer is that critical limit. It is seen that the second transformer provides power just to the 146 EVs at node 634, as shown in Figure 6-3, while all the other EVs (1135) are being supported with power provided from the main transformer. In the figure below, for 19% of power provided for the EVs at each bus bar, the

loading for the main transformer is 97.6%, while for the second transformer it is 106.7%. The second transformer must have no more than 15% power for the 146 EVs at Node 634, to be under critical limits.

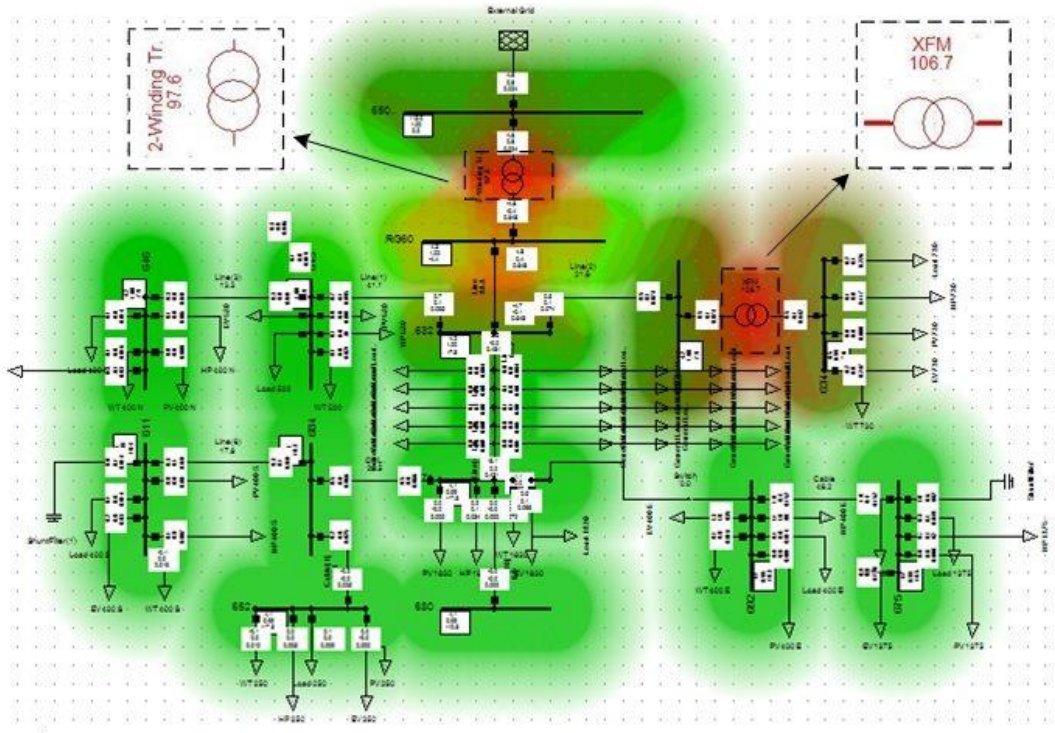


Figure 6-3 Loading difference between the Main and Second Transformer

Because of the reasons mentioned above, for the smart charging case there will use two constraints: the second transformer loading will act as a constraint just for the 146 EVs in node 634, and the main transformer loading for the rest of 1135 EVs.

For the smart charging case, the charging will start from the lowest price hours based on Elspot Market shown in 1.4. On one hand, this maximizes the profit and on the other hand a bigger number of EVs can be charged, due to the system not being so stressed.

In the following table, the maximum energy supported by the transformer (in percentages) for each hour for smart charging are presented, according to the two limits presented above. It can be observed that all the EVs are charged in 7 hours, compared to the dumb charging case where 10 hours are required to fully charge all EVs. Also, because there are now 2 different constraints, for the 1135 EVs, the charging is completed in almost 5 hours, compared to 7 hours for the 146 EVs. The first equation presented below, represents the energy at each hour for 1135 EVs that have as constraint the main transformer.

$$P_{1,max,(t)} = H_{(t)} * EV_{1135} * Ch_p * z_{(t)} \quad (29)$$

The equation presented below represents the energy at each hour for 146 EVs that have as constraint the second transformer.

$$P_{2,max,(i)} = H_{(n)} * EV_{146} * Ch_p * y_{(i)} \quad (30)$$

Table 6-2 Smart Charging % January

SMART CHARGING			
i	Hour based on price (low-high)	Percentage of Max P according to the Main Transformer z_i (%)	Percentage of Max P according to the Second Transformer y_i (%)
1	24	19	15
2	5	22	18
3	1	18	14
4	4	20	16
5	3	20	15
6	2	1	16
7	6	-	6
	Total	100%	100%

In Figure 6-4 the profiles of the main critical limits for smart charging are presented. Due to the charging occurring at the cheaper electricity price hours, which usually occur during the night, the loading of the transformers now is more distributed during the night than in the day. It can be observed now, that the loadings for both transformers are around 100%, compared to the case of dumb charging, where just the second transformer was operating at near 100% loading.

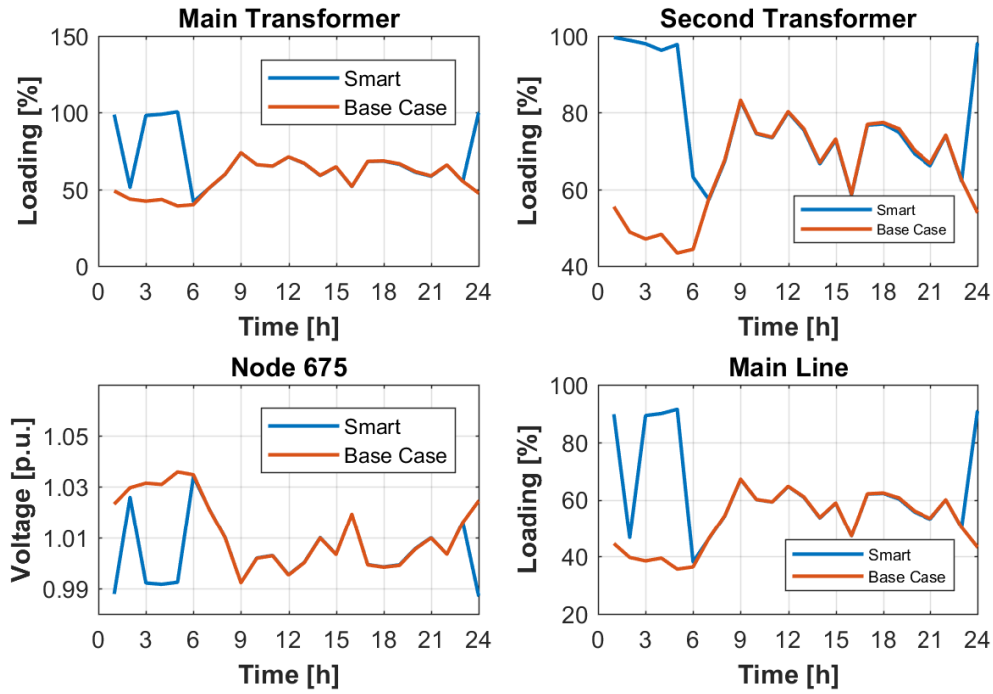


Figure 6-4 Smart Charging Profiles

6.2 July Case

In this subchapter, the dumb charging, as well as the smart charging are analyzed. The renewable integration is the same as in January case, 1 WT and 9 PV at each 105 Houses.

In the table below Table 6-3, the maximum energy supported by the transformer (in percentages) for dumb and smart charging is presented. Same as in January case, the constraint for dumb charging is just the second transformer's loading. For smart charging the constraint is divided between the two transformers' loading. For the 146 EVs (node 634) the second transformer loading acts like a constraint. For the rest of the EVs at the other busbars, the main transformer loading acts as a constraint. For dumb charging, the time needed to fully charge all EVs is 9 hours, while for smart charging case it is completed two times faster, meaning 5 hours.

Table 6-3 Dumb Charging % July

JULY					
	DUMB CHARGING		SMART CHARGING		
i	Hour (i)	Percentage of Max P according to the Second Transformer (x_i) (%)	Hour based on price (low-high) (i)	Percentage of Max P according to the Main Transformer (z_i) (%)	Percentage of Max P according to the Second Transformer (y_i) (%)
1	17	8	6	26	23
2	18	7	5	25	22
3	19	7	4	25	22
4	20	10	24	21	17
5	21	12	3	3	16
6	22	13	-	-	-
7	23	16	-	-	-
8	24	17	-	-	-
9	1	10	-	-	-
	Total	100	Total	100	10

In the following Figure 6-5, profiles of the main critical components of the system are presented for both dumb and smart charging. Regarding the first subplot, for dumb charging case, the main transformer does not reach 100%, showing that for dumb charging this component is not the critical limit that sets the percentage. For smart charging, the main transformer reaches near 100% at midnight, and in the period between 3 to 6, representing the lowest price hours for that day. The same pattern can be observed at the second transformer, but for a longer period. In dumb charging, the second transformer loading is constant at 100%, proving that this limit is the critical one, and all the percentages are set accordingly to it. For the voltage subplot, it can be observed a decrease in voltage each hour the EVs are plugged in, but overall the voltage doesn't violate any constraint. Regarding the main line, it is observed an increase in loading. During the smart charging, when the main transformer is operating near 100% loading, the main line limit loading is as well near the critical point. Comparing to dumb charging, the main transformer is operating at 90%, the main line loading being in this case at around 80%.

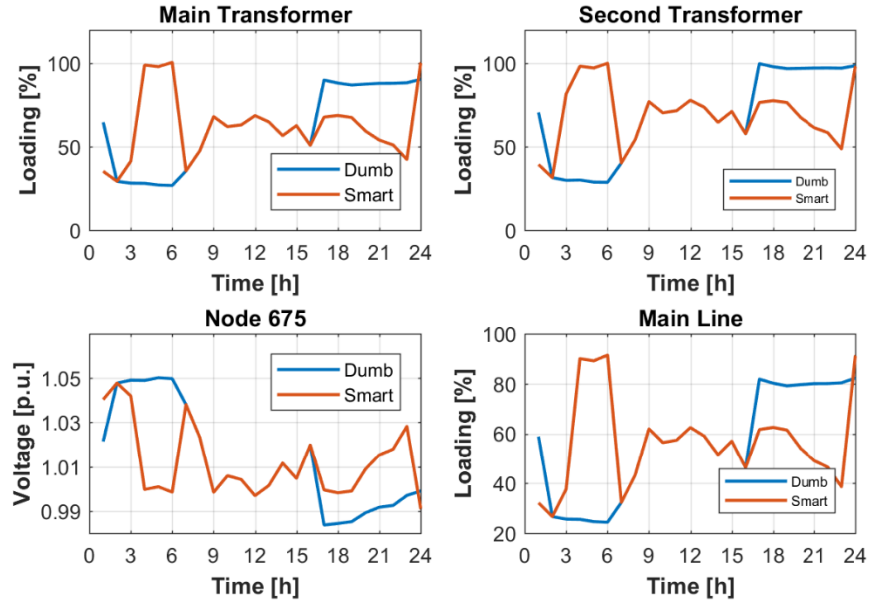


Figure 6-5 Dumb charging profiles- July

6.3 Economic Analysis

6.3.1 January Case

This subchapter is conducted to show the economic benefits of the smart charging. Not only that with smart charging, the EVs can be charged faster (5 hours vs 10 hours) but because of the electricity prices being cheaper during the night, the customer has also the benefit of gaining a profit.

First the charging cost of the dumb charging case is determined, using the below equation:

$$C_D = \sum_{i=17}^n x_i * EV * Ch_p * p_i \quad (31)$$

Where p_i is the price of electricity for hour (i) and x_i is the percentage of energy the system supports for hour (i).

Below, the smart charging cost is presented:

$$C_S = \sum_k^n z_k * EV_1 * Ch_p * p_i + \sum_k^n y_k * EV_2 * Ch_p * p_i \quad (32)$$

Where EV_1 is the number of EVs that have as the limit, the loading of the main transformer (1135 EVs); EV_2 corresponds to the number of EVs that have as the limit the loading of the second transformer (146 EVs) and k is the hour at which the lowest price occurs; Z_i corresponds to the percentage of energy at every busbar, (except for the busbar at the node 634), allowed by the system at hour (i); y_i represents the percentage of energy allowed by the second transformer for busbar 634, at hour (i).

To see the profit, the cost of smart charging is subtracted from the cost of dumb charging, as shown in the following equation.

$$(C_D - C_S) * 360 = 184940 \text{DKK Profit} \quad (33)$$

As shown above, for the whole system the profit is 184 940 DKK for one year. For each vehicle the profit would be for approximately 150 DKK per year.

6.3.2 July Case

For July case using the same equations, presented above, it was found that the profit for one year is 144 570 DKK, for the whole system. For one EV the profit is 112 DKK per year. Due to the variations in prices that occur during one year, an average between the two cases, January and July, is done in order to have a more realistic number. Performing the average, it is discovered that the profit is 164 755 DKK for the whole system by using smart charging over dumb charging. Moreover, each EV owner would gain 128 DKK per year.

Realistically, not all the EV owners will perform smart charging due to various reasons. This means that the owners who choose doing it, will charge at the very cheap hours of the night each night, resulting into an even bigger profit. Assuming that only 40% of EV owners (512 EVs) choose to do smart charging, it is discovered that for one year, for July, the profit becomes 127 DKK compared to 112 DKK, and for January it becomes 408 DKK per EV compared to 150 DKK per EV. The average for both cases for one year is 267.5 DKK.

This major increase for January is due to very low prices during the night, compared to the high prices during the day.

6.4 Summary

In this chapter the dumb and smart charging scenarios were analyzed. An algorithm was made to determine the maximum power at each busbar that can be supplied to the EVs.

Performing the algorithm for dumb charging case, it has been seen that the second transformer is the first critical limit to be violated. Moreover, it is seen that having the second transformer loading as the limit, will affect the power for all the other busbars. Acknowledging this for the smart charging case, the limits are separated: the second transformer loading is now being responsible just for the energy at node 634, and the main transformer is responsible for all the other busbars. By doing this, the energy at the other nodes not being affected can charge with approximately 24% (4% more energy each hour than node 634), faster than in dumb charging where only the second transformer limits the energy.

Furthermore, it has been seen that performing the smart charging over the dumb charging, the time needed to charge all EVs is approximately halved.

Regarding the economic analysis, for January case, one EV owner will save 150 DKK per year if he uses smart charging, and 112 DKK for July. Taking into consideration that not all EV owners will smart charge, an assumption is made, and the profit is calculated just for 40% of the EV owners. Doing so, the profit increases for July from 112 DKK to 127 DKK, and for January from 150 DKK to 408 DKK.

7 Conclusion

The objective of this master thesis is to determine the maximum renewable integration of wind and solar power for a residential grid. To maximize this integration, heat pumps, as well as active and reactive power control are added/performed to the system. Furthermore, the electric vehicles charging profiles have been studied technically as well as economically.

In order to get a valid benchmark for this project, IEEE 13 Bus Network has been built in DIgSILENT PowerFactory and successfully validated. The validation is considered successful with approximately 5% deviation from the original IEE 13. Following the validation, the load flow is conducted for 24 hours in two different cases: one day in January (28 January 2013) and one day in July (28 July 2013). These periods have been chosen due to their wind power generation profile, which correspond to the average profile for that season (winter/summer).

The generation of each renewable unit (e.g wind turbine and PV unit) has been determined based on the wind speed and irradiation profiles recorded in Aalborg. For the calculation of heat pump electricity consumption profile, the thermal profile measured is used as an input. The EVs have been modelled as aggregators.

The maximum renewable integration level has been determined by using a 'trial and error' method, in which three constraints have been investigated (transformers loading, voltage at each busbar, and loading of the lines). Four cases have been studied by the "trial and error" method. It has been discovered that for the system to be stable in both cases, 1 WT and 9PVs at 160 houses, totaling 40 WT and 360 PVs, is taken to be the maximum renewable generation for this case.

Further, after the heat pump integration, which has been done just for January, it has been observed that the new maximum renewable generation is 1 WT and 9 PV at every 10 houses. Although, now that January can sustain much more renewable generation, the July case can't. For this reason, the new number of WT is set accordingly to the July case, 1WT :9PVs at 105 houses.

Furthermore, active and reactive power control are conducted for the wind turbines, to establish how much more renewable integration the system supports. For the active power control, a 7% curtailment ratio is taken as the maximum limit. It is found that for this control, the maximum number of Wind turbines to be 600, 1WT at each 10 houses, approximately, totaling a power of 20.7 MW

The reactive power control has the scope to keep the voltage between the limits, while increasing the number of wind turbines, until the transformer limit has been reached. It was found that, the maximum for this control is total power of 54,68 MW from 1368 Wind Turbines.

Regarding the economic analysis of the EVs, it can be concluded that using smart charging is more profitable and the EVs charging time is two time less than in the dumb charging case. Different strategies of charging and the profits were analyzed. If just 40% of all the EV owners charge their EVs smart, the profit that it can be made per EV owner is 267.5 DKK (average between January and July).

The voltage and line loading limits are kept between the boundaries, the only violations occurring at the transformers. Because the second transformer is affected by 146 EVs, but it is reaching the limit faster than the main one, two separate constraints were taken into consideration, in order to allow for the other busbars to charge more. Therefore, the amount of energy usable by the busbars is with 25% more than in just having the second transformer as a constraint.

8 Future Work

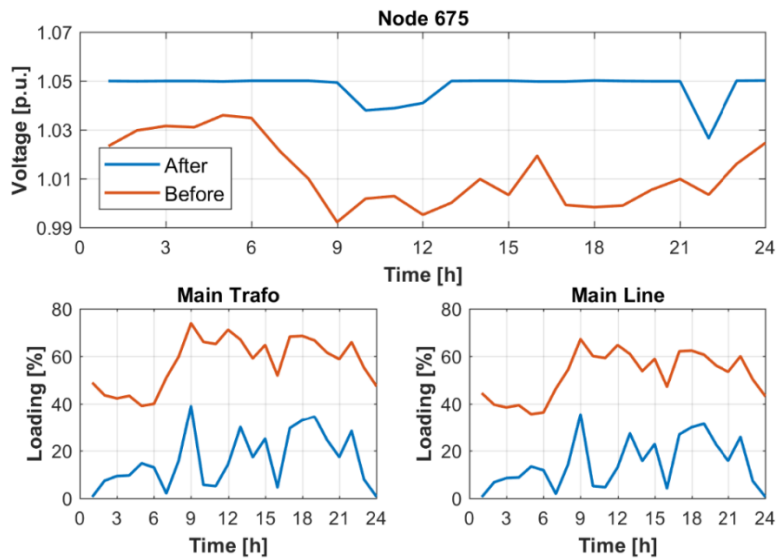
- As shown in the steady state simulations, the transformer tap ratio is one big factor for the small amount of renewable generation available in the night. A tap-control method should be analyzed. By controlling the tap ratio during the night, the renewable generation would increase.
- Due to the fact that the renewable generation is quickly changing during one day, an analysis with a smaller time step should be conducted for better results.
- Considering that this thesis is made for Denmark, which is a country that does not have warm temperatures during the summer, the heat pumps were not included for cooling in July. If this study would be conducted for another region, the study of heat pumps in summer should be analyzed.
- A possibility to regulate the energy market would be by integrating the V2G concept which would also give the possibility to the EV owners to gain more profit other than the one gained from smart charging.
- As seen in reactive power control as well as in EV integration, the main transformer is the component of the system that reaches the limit first. A techno-economic analysis should be conducted to determine if adding one more transformer in parallel to this one would be suitable.
- Power quality problems should be investigated for a better understanding of the system's behavior. Other than this, dynamic simulations should be made, such as transient analysis, for the renewable generation part.

Bibliography

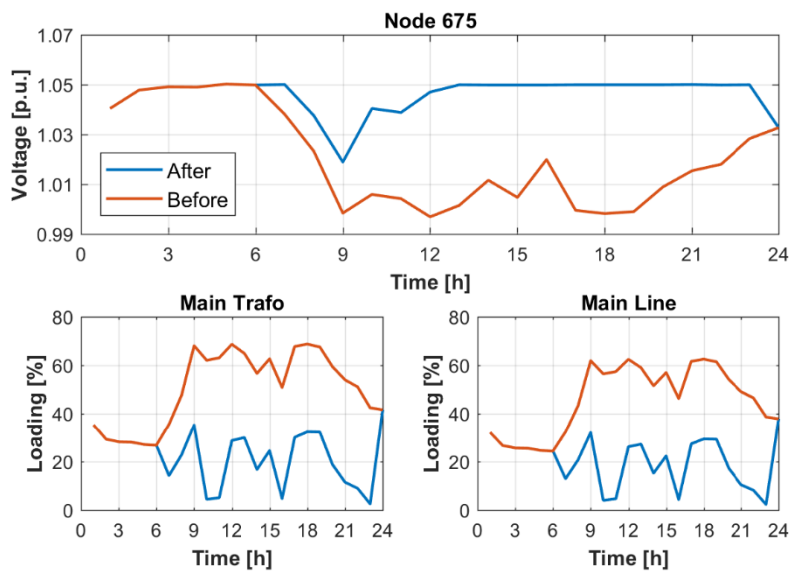
- [1] Anglia Ruskin University, “Country Resource Maps,” 2014.
- [2] United Nations Intergovernmental Panel (IPCC), “Denmark ’ s commitment to 100 % renewable energy,” pp. 1–7, 2014.
- [3] “Renewable Energy Integration,” 2017. .
- [4] Energinet, “Energinet, ‘Danish national transmission system operator.’ [Online].” .
- [5] “‘Annual Report 2015,’ p. 72, 2015.” .
- [6] The Danish Energy Agency, “energy statistics 2013 – data tables statistics and maps.”
- [7] J. Larminie and J. Lowry, *Electric Vehicle Technology Explained*. 2012.
- [8] K. Hedegaard, H. Ravn, N. Juul, and P. Meibom, “Effects of electric vehicles on power systems in Northern Europe,” *Energy*, vol. 48, no. 1, pp. 356–368, 2012.
- [9] and G. E. W. Unter, J. Auer, “‘Integration of Electric Vehicles in the Austrian Electricity System,’ vol. 99, no. 0057254,” 2013.
- [10] D. S. Gautam, F. Musavi, M. Edington, W. Eberle, and W. G. Dunford, “An automotive onboard 3.3-kW battery charger for PHEV application,” *IEEE Trans. Veh. Technol.*, vol. 61, no. 8, pp. 3466–3474, 2012.
- [11] “Sales By 2020, Navigante Search.” .
- [12] “Volvo Stops Production of conventional vehicles.” .
- [13] Forbes, “Volvo will stop produce conventional vehicles by 2019.” .
- [14] AquaNexa, “Air-air Heat Pump Cycle.” .
- [15] Energinet.dk, “Fra vindkraft til varmepumper,” p. 26, 2012.
- [16] “Northeast Energy Efficiency Partnerships.” .
- [17] Eurostat, “Electricity and Natural Gas Prices Statistics,” 2015.
- [18] S. Report, “Supply report 2017,” 2017.
- [19] H. Markiewicz and A. Klajn, “Voltage Disturbances,” *Power Qual. Appl. Guid.*, vol. 5.4.2, pp. 4–11, 2004.
- [20] C. C. C. CCC, “Denmark: a European Smart Grid Hub,” 2011.
- [21] Nordic Energy Regulators, “Economical regulations of electricity grids in Nordic countries,” p. www.nordicenergyregulators.org.
- [22] G. Andersson, “Modelling and analysis of electric power systems,” *EEH-Power Syst. Lab. Swiss Fed. ...*, no. March, 2004.
- [23] B. Espinoza, “Power{ }Systems{ }Anlalysis{ }by{ }Arthur{ }R{ }Bergen-libre.pdf,” *Facultar de Agronomía*. pp. 103–127, 2007.
- [24] J. R. Pillai, “Advance Power System Course,” 2017.
- [25] W. H. Kersting, “Radial distribution test feeders,” *Proc. IEEE Power Eng. Soc. Transm. Distrib. Conf.*, vol. 2, no. WINTER MEETING, pp. 908–912, 2001.
- [26] S. R. Overview, “SolarGIS ® Report,” pp. 1–9, 2014.
- [27] “‘Nordisk Folkecenter for vedvarende energi.’ [Online],” p. http://www.folkecenter.dk/dk/rd/vindkraft/smaa_vin.
- [28] “‘Osiris Energy.’ [Online].,” p. <http://www.osirisenergy.com/>.
- [29] Natural Resources Canada, *Commercial Earth Energy Systems: A buyer’s guide*. 2002.
- [30] K. Katsavounis, P. Hou, W. Hu, and Z. Chen, “Optimized Control of a Residential Heat

- Pump,” 2017.
- [31] ““Danish Energy Agency.”[Online].” .
 - [32] Z. LIU, Q. WU, L. CHRISTENSEN, A. RAUTIAINEN, and Y. XUE, “Driving pattern analysis of Nordic region based on National Travel Surveys for electric vehicle integration,” *J. Mod. Power Syst. Clean Energy*, vol. 3, no. 2, pp. 180–189, 2015.
 - [33] “Tesla Cars Charging Power,” p. www.tesla.com.
 - [34] I. I. E. V. and C. Engineering, “Types of Charging,” 2012.
 - [35] “Three European Domestic Electrical Consumption Profiles,” 2006.
 - [36] Danish Energy Agency, *Denmark’s Energy and Climate Outlook 2017*. 2017.
 - [37] A. E. G. For and R. E. By, “powE[R] 2030,” 2014.

Appendix 1



The voltage and line/trafo loading is presented for January, where 3600 Wind Turbines are integrated.



The voltage and line/trafo loading is presented for July where 3600 Wind turbines are integrated.